Adaptive Super Twisting Sliding Mode Formation Control of Multiple Quad-rotors with Wind Disturbances

Author

Yasir Mehmood

Registration Number

318899

Supervisor

Dr. Jawad Aslam

DEPARTMENT

SCHOOL OF MECHANICAL & MANUFACTURING ENGINEERING

NATIONAL UNIVERSITY OF SCIENCES AND TECHNOLOGY

ISLAMABAD

APRIL, 2021

Adaptive Super Twisting Sliding Mode Formation Control of Multiple Quad-rotors with Wind Disturbances

Author

Yasir Mehmood

Regn Number

318899

A thesis submitted in partial fulfillment of the requirements for the degree of

MS Mechanical Engineering

Thesis Supervisor:

Dr. Jawad Aslam

Thesis Supervisor's Signature: _____

DEPARTMENT

SCHOOL OF MECHANICAL & MANUFACTURING ENGINEERING

NATIONAL UNIVERSITY OF SCIENCES AND TECHNOLOGY,

ISLAMABAD

APRIL, 2021

Declaration

I certify that this research work titled "*Adaptive Super Twisting Sliding Mode Formation Control of Multiple Quad-rotors with Wind Disturbances"* is my own work. The work has not been presented elsewhere for assessment. The material that has been used from other sources it has been properly acknowledged / referred.

Signature of Student

2021-NUST-MS-Mech-318899

Plagiarism Certificate (Turnitin Report)

This thesis has been checked for Plagiarism. Turnitin report endorsed by Supervisor is attached.

Signature of Student

Registration Number: 318899

Signature of Supervisor

Copyright Statement

- Copyright in text of this thesis rests with the student author. Copies (by any process) either in full, or of extracts, may be made only in accordance with instructions given by the author and lodged in the Library of NUST School of Mechanical & Manufacturing Engineering (SMME). Details may be obtained by the Librarian. This page must form part of any such copies made. Further copies (by any process) may not be made without the permission (in writing) of the author.
- The ownership of any intellectual property rights which may be described in this thesis is vested in NUST School of Mechanical & Manufacturing Engineering, subject to any prior agreement to the contrary, and may not be made available for use by third parties without the written permission of the SMME, which will prescribe the terms and conditions of any such agreement.
- Further information on the conditions under which disclosures and exploitation may take place is available from the Library of NUST School of Mechanical & Manufacturing Engineering, Islamabad.

Acknowledgements

I am thankful to my Creator Allah Subhana-Watala to have guided me throughout this work at every step and for every new thought which You setup in my mind to improve it. Indeed, I could have done nothing without Your priceless help and guidance. Whosoever helped me throughout the course of my thesis, whether my parents or any other individual was Your will, so indeed none be worthy of praise but You.

I am profusely thankful to my beloved parents who raised me when I was not capable of walking and continued to support me throughout in every department of my life.

I would also like to express special thanks to my supervisor Dr. Jawad Aslam for his help throughout my thesis and also for Advanced Control Systems and Advanced Modeling and Simulations courses which he has taught me. I can safely say that I haven't learned any other engineering subject in such depth than the ones which he has taught.

I would also like to pay special thanks to Dr. Nasim Ullah for his tremendous support and cooperation. Each time I got stuck in something, he came up with the solution. Without his help I wouldn’t have been able to complete my thesis. I appreciate his patience and guidance throughout the whole thesis.

I would also like to thank Dr. Rehan Zahid, Dr. Riaz Ahmad Mufti and Dr. Emad Uddin for being on my thesis guidance and evaluation committee and express my special thanks to Dr. Mian Ashfaq Ali for his help. I am also thankful to Mr. Fazal Badshah for their support and cooperation.

Finally, I would like to express my gratitude to all the individuals who have rendered valuable assistance to my study.

Dedicated to my exceptional parents and adored siblings whose tremendous support and cooperation led me to this wonderful accomplishment.

Abstract

In recent times, multiple unmanned aerial vehicles (UAVs) grouped as leader follower configuration have found numerous applications in various areas such as surveillance, industrial automation and disaster management. The accuracy and reliability for performing such crucial tasks in a group is highly dependent on the applied control strategy. The formation and trajectories of multiple UAVs are governed by two separate controllers, namely formation and trajectory tracking controllers respectively. Environmental effects, disturbances due to wind and parametric uncertainties make the controller design process as a challenging task. This article proposes a robust adaptive formation and trajectory tacking control of multiple quad-rotor UAVs using super twisting sliding mode control method. In the proposed design, Lyapunov function based adaptive disturbance estimators are used to compensate the effects of the disturbances due to wind and parametric uncertainties. The stability of the proposed controllers is guaranteed using Lyapunov theorems. Two variants of the control schemes namely fixed gain super twisting SMC (STSMC) and adaptive super twisting SMC (ASTSMC) are tested using numerical simulations performed in MATLAB/Simulink. From the results presented, it is verified that ASTSMC scheme exhibits enhanced robustness as compared to the fixed gain STSMC.

Key Words: *Quad-rotor control, adaptive robust control, super twisting sliding mode control, formation control*

Table of Contents

Declaration ..... **i**
Plagiarism Certificate (Turnitin Report) ..... **ii**
Copyright Statement ..... **iii**
Acknowledgements ..... **iv**
Abstract ..... **vi**
Table of Contents ..... **vii**
List of Figures ..... **viii**
List of Tables **1**
CHAPTER 1: INTRODUCTION **2**
1.1 Background, Scope and Motivation 2
1.2 Aim of the thesis 4
1.3 Nomenclature 5
CHAPTER 2: SYSTEM DESCRIPTION AND MATHEMATICAL MODELLING **6**
2.1 Quadcopter Dynamics Model 6
2.2 Formation Error Dynamics Model 7
CHAPTER 3: TRAJECTORY AND FORMATION CONTROLLERS FORMULATION **9**
3.1 LEADER UAV CONTROL FORMULATION 10
Attitude Control: 10
Altitude and position Control: 12
3.2 LEADER FOLLOWER FORMATION CONTROL 17
3.3 FOLLOWER UAVs CONTROL FORMULATION 18
CHAPTER 4: RESULTS AND DISCUSSIONS **19**
CHAPTER 5: CONCLUSIONS **31**
APPENDIX A: SIMULINK® BLOCK MODEL AND MATLAB FUNCTION CODES **32**
REFERENCES **39**

List of Figures

Figure 1: Quad-rotor in inertial reference frame 6
Figure 2: Leader-Follower Configuration.....7
Figure 3: Applied acceleration type disturbance in X and Y dynamics 20
Figure 4: XYZ trajectory tracking comparison under wind disturbance 22
Figure 5: XY leader trajectory tracking comparison under wind disturbance.....23
Figure 6: XY follower 1 trajectory tracking comparison under wind disturbance 23
Figure 7: XY follower 2 trajectory tracking comparison under wind disturbance 24
Figure 8: XY Leader-followers trajectory tracking comparison under wind disturbance 24
Figure 9: $Xleader$ tracking comparison under wind disturbance 25
Figure 10: $Yleader$ tracking comparison under wind disturbance.....25
Figure 11: $XF1$ tracking comparison under wind disturbance.....26
Figure 12: $YF1$ tracking comparison under wind disturbance.....27
Figure 13: $XF2$ tracking comparison under wind disturbance.....27
Figure 14: $YF2$ tracking comparison under wind disturbance.....27
Figure 15: θ tracking comparison under wind disturbance.....28
Figure 16: ϕ tracking comparison under wind disturbance.....28
Figure 17: Difference between desired θ, ϕ with ASTSMC and STSMC controllers.....29
Figure 18: z tracking 29
Figure 19: ψ tracking.....29
Figure 20: Formation controller tracking 30
Figure 21: Control inputs using proposed control scheme 30
Figure 22: Simulink Model for swarm of 3 quad-copters.....32
Figure 23: Reference X, Y and Z position of leader quad-copter.....33
Figure 24: Position Controller for Leader quad-rotor.....33
Figure 25: Attitude Controller for roll, pitch and yaw angles for leader quad-copter 34
Figure 26: Altitude Controller of leader quad-copter 34
Figure 27: Dynamics model of leader quad-copter.....35
Figure 28: Motor Mixing Algorithm of leader quadcopter.....35
Figure 29: Rotational Dynamics of leader quadcopter 36
Figure 30: Translational Dynamics of leader quadcopter.....36

List of Tables

Table 1: Leader-followers UAV parameters.....21
Table 2: Leader UAV control parameters for attitude, altitude and position loops 21
Table 3: Follower UAVs control parameters for attitude, altitude and position loops. 22

CHAPTER 1: INTRODUCTION

The research work in this dissertation has been presented in four parts. First part is related to system description and mathematical modeling. The objective of this part is the modelling of a single quad-copter and translational dynamics of multiple UAVs. The second part includes the trajectory and the formation controller formulation. Then the simulation results are presented and comparative analysis for different controllers is done. At last, conclusions are made.

1.1 Background, Scope and Motivation

A flight in which more than one quad-rotors fly and maintain the relative distance among each other is called formation flight. In recent times, the interest in the formation control of quad-rotors has attracted a lot of attention. This trend is due to its potential applications in defense industry, aerial mapping, search and rescue operations, oil fields monitoring, agriculture and transportation of suspended loads [1]. It is expected that by 2027 the payload market value of global UAV may reach USD 3 billion due to its anticipated usefulness [2]. Multiple quad-copters increases the capacity for equipping sensors, provides larger payload capacity as compared to single quad-copter [3-7]. However, controlling the formation of multiple quad-rotors in the presence of uncertainties is a challenging task. Moreover, the derivation of formation dynamic model for multiple UAVs in presence of external perturbations has also become an important topic.

The transnational and rotational dynamics of a quad rotor is modeled as six degree of freedom nonlinear differential equations [8-11]. For multiple UAVs, different formation geometries exist depending upon the number of quad-rotors and the purpose of flight. These include V shape geometry and finger four geometry. V shape geometry is used in this paper for flight formation of 3 quad-copters. Since a quad-copter is a complex system with under-actuated multi variable non-linear model hence its formation control problem is more difficult to control. In order to ensure robust formation control, the modeling uncertainties and the disturbance due to wind gust must be compensated using appropriate control schemes.

To solve the formation control problem of the quad rotor, many research efforts have been made. In [12] the authors proposed a leader–follower formation control using classical proportional derivative scheme and fuzzy logic system for the formation pattern. However, the above controller did not take uncertainties into considerations. In [13], a prescribed performance

controller is proposed for formation control of multiple UAVs. The prescribed performance controller ensures robust formation pattern and trajectory. In [14], a classical PID control scheme with a sliding mode controller (SMC) is proposed for multiple quad-rotors. However, the above mentioned PID-SMC controller ignores the disturbances and communication delays between multiple UAVs. In [15-17], classical SMC method is proposed for formation control problems of multiple UAVs, however the classical SMC method offers high frequency chattering in the excitation signal. Chattering phenomena degrades the life of the actuators. A control scheme for the circular formation scheme of multiple UAVs is presented in [18]. A classical PI control based synchronization control for the formation of two UAVs is presented in [19]. In [20] a distributed controller is presented to compensate the communication delays in multiple UAVs formation. Similarly, a nonlinear distributed controller is proposed for formation of micro UAVs [21]. In [22], the authors proposed a cohesive formation controller for multiple UAVs. A back-stepping control scheme is proposed for the formation control of multiple UAVs [23]. Similarly, a model predictive control scheme is proposed for multiple UAVs using adaptive gain tuning method in [24-25]. Velocity tracking and formation control of quad-copters is achieved by the design of priori-bounded intermediary adaptive controller which gives the reference orientation and bounded control thrust [26]. A guidance algorithm based on Lyapunov function is used for the formation control of quad-rotors with attached slung load, where the quad-copters are controlled using linear quadratic tracking controller [27]. Leader follower formation controller is designed for two parrot drones in [28], where a proportional derivative controller is implemented in the respective models. The problems related to formation and tracking control of quad-copters in leader follower formation are addressed and a formation controller is designed to avoid collision in swarm [29]. Adaptive law for the formation control of swarm UAVs in leader follower mechanism influenced by motion constraints and unknown external disturbances is discussed in [30]. For a swarm of three quad-rotors, a model reference adaptive control algorithm is presented in [31]. The controller gains are tuned online, by which the algorithm allows the system to adapt to unexpected disturbances. However, in this method, no robust controller is investigated. A semi physical platform for formation control of multiple fixed wings UAV is proposed in [33]. In [34], a detailed survey on low-cost UAV platforms for infra structure monitoring is proposed.

The above cited work is specifically focused on the formation control of multiple UAVs. It is also necessary to describe the back ground of robust control system due to its utmost

importance in control community. Robust control is designed for uncertain systems in which the uncertainty belongs to bounded set [35]. Robust controllers are designed both in frequency and time domains. A widely utilized frequency domain robust controller is the H_∞method and it was first reported in [35]. Later on, several variants of H_∞ control were reported in the literature such as loop shaping in [36], optimal H_∞ control using Riccati equations [37] and Linear Matrix Inequalities (LMIs) based design in [38]. In frequency domain, the performance and stability of the control system is measured in terms of gain and phase margins, percent overshoot, rise, delay and settling times of the signals. Apart from frequency domain, a modern approach for designing robust controllers is the state space frame work. Sliding mode based control (SMC) system variants are the most widely utilized methods and it find numerous applications in all areas of science and technology [39]. Classical SMC has several disadvantages such as high frequency chattering and asymptotic convergence property. These shortcomings are addressed by introducing new variants of SMC such as global sliding mode [40], LMI based SMC [41], Higher order SMC [42-43], Lyapunov based adaptive SMC and Non-singular terminal SMC in [44]. A widely and important criteria to ensure the stability of the SMC controllers is the Lyapunov theorem [45]. The proposed theorems ensure global stability of the nonlinear systems and control using the condition that the disturbances are bounded.

1.2 Aim of the thesis

Considering the aforementioned literature review, this paper proposes adaptive robust formation and trajectory tracking of multiple UAVs using super-twisting sliding mode control method. The proposed controller compensates the disturbances using adaptive control laws derived by Lyapunov function method. System stability is ensured using Lyapunov theorem. Furthermore, the formation flight between multiple UAVs are also controlled using super twisting sliding mode control methods. Following specific contributions are highlighted:

1. In presence of external disturbances, robust formation and trajectory tracking of multiple UAVs is achieved using adaptive super twisting sliding mode control method.
2. The adaptive laws are derived using Lyapunov theorem and implemented using projection operators.

1.3 Nomenclature

d_{Xi}	Uncertainty in $\ddot{X}$ dynamics of ith quad-rotor [m/sec^2]
$\ddot{X}_i$, $\ddot{Y}_i$, $\ddot{Z}_i$	Accelerations of ith quad-rotor in earth coordinates [m/sec^2]
$\dot{X}_i$, $\dot{Y}_i$, $\dot{Z}_i$	Velocity of ith quad-rotor in earth coordinates [m/sec]
Ω_{ri}	Overall speed of the propellers of ith quad-rotor [rad=sec]
φ_i	Roll angle of ith quad-rotor [rad]
ψ_i	Yaw angle of ith quad-rotor [rad]
θ_i	Pitch angle of ith quad-rotor [rad]
d_{Yi}	Uncertainty in $\ddot{Y}$ dynamics of i_{th} quad-rotor [m=sec^2]
g	Acceleration due to gravity [m=sec^2]
I_{xi}, I_{yi}, I_{zi}	Moments of ith quad-rotor inertia in X, Y and Z coordinates [Kg-m^2]
J_{ri}	Rotor inertia of ith quad-rotor [Kg-m^2]
$M_{\varphi i}$	Roll moment of ith quad-rotor [N-m]
$M_{\theta i}$	Pitch moment of ith quad-rotor [N-m]
m_{Qi}	Mass of ith quad-rotor [Kg]
X_i, Y_i, Z_i	Position of ith quad-rotor in earth coordinates [m]

CHAPTER 2: SYSTEM DESCRIPTION AND MATHEMATICAL MODELLING

2.1 Quadcopter Dynamics Model

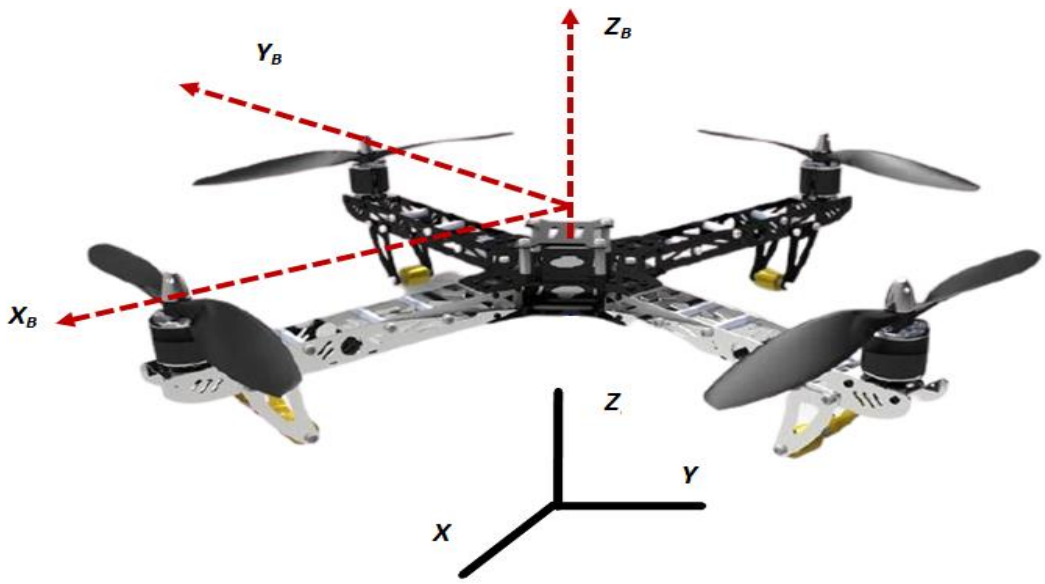

Figure 1: Quad-rotor in inertial reference frame

Fig. 1 shows a quad-rotor UAV in earth's reference coordinates (X, Y, Z). Apart from inertial frame of reference, the body coordinates of the UAV are given as: (X_B Y_B Z_B). To derive the model, the following assumptions are made.

Assumption 1: It is assumed that the UAVs are represented by a symmetrical rigid body configuration with masses m.

Assumption 2: The external disturbances affect the X and Y accelerations components of each UAV.

Assumption 3: It is assumed that the disturbances are affecting the leader and followers UAV uniformly.

Based on the above assumptions, the dynamic model of the multiple UAV quad-rotors is formulated as 6 degree of freedom equations. The dynamic equations expressing the linear and angular dynamics of the quad-rotors are given as follows:

$$\ddot{X}_i = (\sin\psi_i \sin\phi_i + \cos\psi_i \sin\theta_i \cos\phi_i)\frac{U_{1i}}{m_{Qi}} - D_{Xi} \qquad (1)$$

$$\ddot{Y}_i = (-\cos\psi_i \sin\phi_i + \sin\psi_i \sin\theta_i \cos\phi_i)\frac{U_{1i}}{m_{Qi}} - D_{Yi} \tag{2}$$

$$\ddot{Z}_i = g - (\cos\theta_i \cos\phi_i)\frac{U_{1i}}{m_{Qi}} - D_{Zi} \tag{3}$$

$$\ddot{\phi}_i = \frac{I_{yi} - I_{zi}}{I_{xi}}\dot{\theta}_i\dot{\psi}_i - \frac{J_{ri}}{I_{xi}}\dot{\theta}_i\Omega_{ri} + \frac{l_i}{I_{xi}}U_{2i} - D_{\phi_i} \tag{4}$$

$$\ddot{\theta}_i = \frac{I_{zi} - I_{xi}}{I_{yi}}\dot{\phi}_i\dot{\psi}_i - \frac{J_{ri}}{I_{yi}}\dot{\phi}_i\Omega_{ri} + \frac{l_i}{I_{yi}}U_{3i} - D_{\theta_i} \tag{5}$$

$$\ddot{\psi}_i = \frac{I_{xi} - I_{yi}}{I_{zi}}\dot{\phi}_i\dot{\theta}_i + \frac{l_i}{I_{zi}}U_{4i} - D_{\psi_i} \tag{6}$$

Equations. 1-6 formulates the mathematical model of multiple quad-rotors UAV. From Eq. 1-6, D_{Xi} and D_{Yi} represent the uncertainty in X and Y acceleration channels, while i is an index representing [L, j] and j = [F1, F2]. The subscript L represents the leader UAV, while F1 and F2 show follower 1 and 2 UAVs respectively.

2.2 Formation Error Dynamics Model

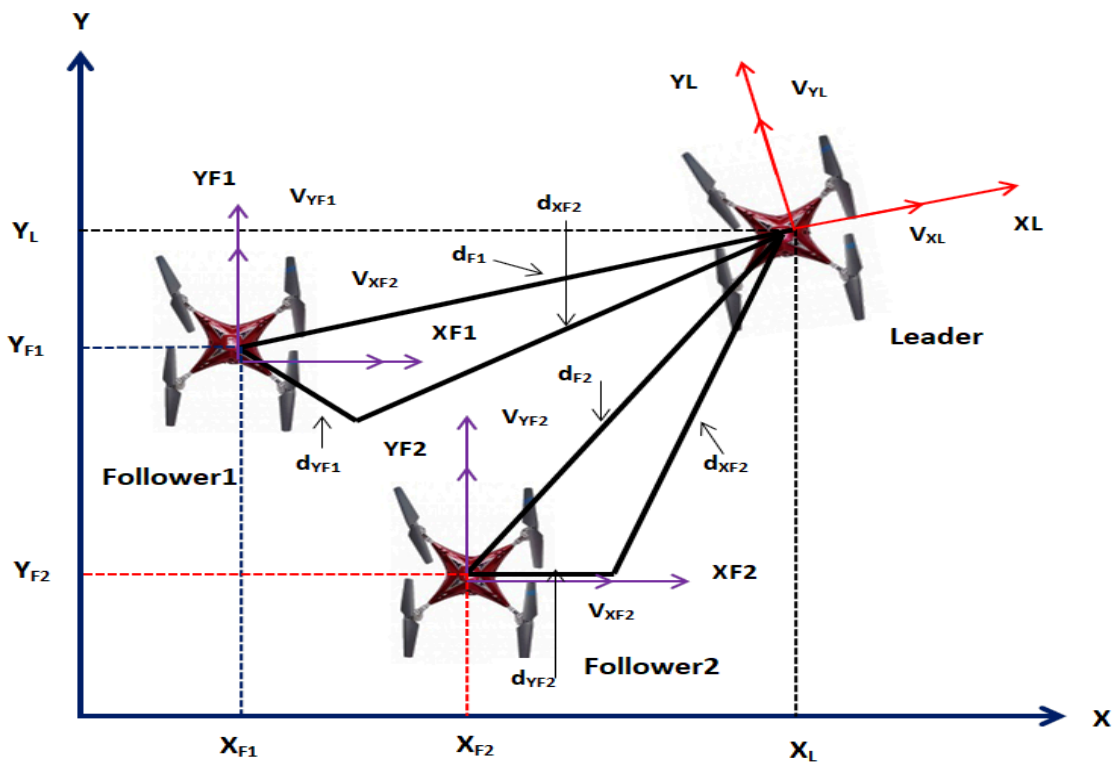

Figure 2: Leader-Follower Configuration

Figure 2 shows multiple UAV quad-rotors in leader follower configuration. Referring to Fig. 2, the transnational dynamics of the UAVs are expressed as follows:

$$\dot{X}_i = V_{Xi}\cos(\psi_i) - V_{Yi}\sin(\psi_i) \tag{7}$$

$$\dot{Y}_i = V_{Xi}\sin(\psi_i) + V_{Yi}\cos(\psi_i) \tag{8}$$

$$\dot{\psi}_L = \omega_L \tag{9}$$

Where V_{Xi} and V_{Yi} represents the velocities in X and Y directions of the inertial frame. As shown in Fig. 2, let the follower UAVs maintain d_{Xj} and d_{Yj} distances in X and Y planes respectively with respect to the leader UAV, so d_{Xj} and d_{Yj} are expressed as follows:

$$d_{Xj} = -\left(X_L - X_j\right)\cos(\psi_L) - \left(Y_L - Y_j\right)\sin(\psi_L) \tag{10}$$

$$d_{Yj} = \left(X_L - X_j\right)\sin(\psi_L) - \left(Y_L - Y_j\right)\cos(\psi_L) \tag{11}$$

Where $d_{Xj} = d_i cos(\phi), d_{Yj} = d_i sin(\phi)$ and $X_j = [X_{F1},\ X_{F2}]$, the error in ψ dynamics as defined as follows: $e_\psi = \psi_j - \psi_L$. By taking the first derivatives of Eqs. 10-11 with respect to time and combining the resultant expressions with Eqs.7-8 yields the following expressions:

$$\dot{d_{XJ}} = d_{Yj}\omega_L + V_{Xj}\cos\left(e_\psi\right) - V_{Yj}\sin\left(e_\psi\right) - V_{XL} \tag{12}$$

$$\dot{d_{YJ}} = -d_{Xj}\omega_L + V_{Xj}\sin e_\psi + V_{Yj}\cos e_\psi - V_{YL} \tag{13}$$

Where V_{Xj}, V_{Yj}, V_{XL} and V_{YL} represent the longitudinal and lateral velocities of the follower 1, follower 2 and leader UAVs respectively. By defining errors in the longitudinal and lateral dynamics of Eq. 12-13, the error state equation is represented as follows:

$$\dot{\chi} = F(\chi) + G(\chi)v \tag{14}$$

Eq. 14 are explained as follows:

$$\chi = \begin{bmatrix} e_{Xj} \\ e_{Yj} \\ e_\psi \end{bmatrix};\ \dot{\chi} = \begin{bmatrix} \dot{e_{XJ}} \\ \dot{e_{YJ}} \\ \dot{e_\psi} \end{bmatrix};\ v = \begin{bmatrix} V_{Xj} \\ V_{Yj} \\ \omega_F \end{bmatrix} \tag{15}$$

Also, the terms $G(\chi)$ and $F(\chi)$ are expressed as follows:

$$F(\chi) = \begin{bmatrix} e_{Yj}\omega_L + V_{XL} - \omega_L d_{Yj}^d \\ -e_{Xj}\omega_L + V_{YL} + \omega_L d_{Xj}^d \\ e_\psi \end{bmatrix} \tag{16}$$

$$G(\chi) = \begin{bmatrix} -ce_\psi & se_\psi & 0 \\ -se_\psi & -ce_\psi & 0 \\ 0 & 0 & 1 \end{bmatrix} \tag{17}$$

In Eq. 17, e_ψ is already defined, while c represents cos while s is a sin function. Also form Eq. 15, we define: $e_{Xj} = {d_{Xj}}^d - d_{Xj}\ and\ e_{Yj} = {d_{Yj}}^d - d_{Yj}$. Where ${d_{Xj}}^d$ and ${d_{Yj}}^d$ represent the desired commands. Finally, the desired reference trajectories for follower UAVs

are expressed as follows:

$$\begin{aligned} X_{dj} &= X_L - d_{Xj}\cos(\psi_L) - d_{Yj}\sin(\psi_L) \\ Y_{dj} &= Y_L + d_{Xj}\sin(\psi_L) + d_{Yj}\cos(\psi_L) \end{aligned} \tag{18}$$

CHAPTER 3: TRAJECTORY AND FORMATION CONTROLLERS FORMULATION

In this section as a first step, the derivations of the attitude, altitude and position controllers are formulated for the leader UAV. As a second step, the formation controller is derived and based on it, new references are calculated for follower 1 and follower 2 UAVs. In the last step, the trajectory and attitude controllers of the leader UAV are generalized for follower UAVs. Before deriving the control schemes, the following assumptions are made:

Assumption 4: It is assumed that the following condition is true for the uncertainty terms:

$$\left||D_{Xi}|\right| \leq \Delta_{1i};\ \left||D_{Yi}|\right| \leq \Delta_{2i};\ \left||D_{Zi}|\right| \leq \Delta_{3i};\ \left|\left|D_{\phi_i}\right|\right| \leq \Delta_{4i}\ ;\left|\left|D_{\theta_i}\right|\right| \leq \Delta_{5i}\ ;\left|\left|D_{\psi_i}\right|\right| \leq \Delta_{6i}$$

Where Δ_{1i}, Δ_{2i}, Δ_{3i}, Δ_{4i}, Δ_{5i}, Δ_{6i} represent the upper bound of the mentioned uncertainties.

3.1 LEADER UAV CONTROL FORMULATION

In this subsection the attitude, altitude and position controllers are derived for leader UAV using adaptive super twisting sliding mode control method.

Attitude Control:

Attitude controllers regulate the roll, yaw and pitch angles of the UAV. Let the reference Euler angle commands for the leader UAV are set as ϕ_{dL}, θ_{dL}, ψ_{dL}, then the desired sliding manifold is chosen as follows:

$$S_{\phi_L} = k_1 e_{\phi_L} + k_2 \dot{e}_{\phi_L} \tag{19}$$

Where S_{ϕ_L} represents the sliding surface for ϕ_L loop, k_1, k_2 are the design constants and the ϕ_L loop error dynamics are expressed as follows i.e., $e_{\phi_L} = \phi_L - \phi_{dL},\ \dot{e}_{\phi_L} = \dot{\phi}_L - \dot{\phi}_{dL}$. By taking the first time derivative of Eq. 19, the following expression is obtained:

$$\dot{S}_{\phi_L} = k_1 \dot{e}_{\phi_L} + k_2 \ddot{e}_{\phi_L} \tag{20}$$

Eq. 4 and Eq. 20 are combined and expressed as follows:

$$\dot{S}_{\phi_L} = k_1 \dot{e}_{\phi_L} + k_2 \left[a_{1L}\theta_L \dot{\psi}_L - a_{2L}\dot{\theta}_L \Omega_{rL} + b_{1L} U_{2L} - D_{\phi_L} - \ddot{\phi}_{dL}\right] \tag{21}$$

In Eq. 21, the coefficients are defined as follows, i.e., $a_{1L} = \frac{I_{yL} - I_{zL}}{I_{xL}},\ a_{2L} = \frac{J_{rL}}{I_{xL}},\ b_{1L} = \frac{l}{I_{xL}}$; then the equivalent control law for ϕ_L loop is derived as follows:

$$U_{2Leq} = \frac{1}{b_{1L}}\left(\frac{-k_1}{k_2}\dot{e_{\phi_L}} - a_{1L}\dot{\theta_L}\dot{\psi_L} + a_{2L}\dot{\theta_L}\Omega_{rL} + \ddot{\phi_{dL}}\right) \tag{22}$$

Using super twisting algorithm, the switching control law is derived as follows:

$$U_{2Lsw} = \frac{-k_{d1}}{b_{1L}}\left|S_{\phi_L}\right|^{0.5} sgn\left(S_{\phi_L}\right) - \frac{k_{d2}}{b_{1L}}\int sgn\left(S_{\phi_L}\right) \tag{23}$$

Referring to Eq. 22 and 23, the total control action is the sum of equivalent and switching control parts i.e., $U_{2L} = U_{2Leq} + U_{2Lsw}$. Similar procedure is adopted to derive the pitch and yaw controllers. The sliding surfaces for θ_L and ψ_L loops are defined as follows i.e., $S_{\theta_L} = k_3 e_{\theta_L} + k_4 \dot{e_{\theta_L}}$ and $S_{\psi_L} = k_5 e_{\psi_L} + k_6 \dot{e_{\psi_L}}$, then the θ_L and ψ_L loops controllers are formulated as follows:

$$U_{3Leq} = \frac{1}{b_{2L}}\left(\frac{-k_3}{k_4}\dot{e_{\theta_L}} - a_{3L}\dot{\phi_L}\dot{\psi_L} + a_{4L}\dot{\phi_L}\Omega_{rL} + \ddot{\theta_{dL}}\right) \tag{24}$$

$$U_{3Lsw} = \frac{-k_{d3}}{b_{2L}}\left|S_{\theta_L}\right|^{0.5} sgn\left(S_{\theta_L}\right) - \frac{k_{d4}}{b_{2L}}\int sgn\left(S_{\theta_L}\right) \tag{25}$$

$$U_{4Leq} = \frac{1}{b_{3L}}\left(\frac{-k_5}{k_6}\dot{e_{\psi_L}} - a_{5L}\dot{\phi_L}\dot{\theta_L} + \ddot{\psi_{dL}}\right) \tag{26}$$

$$U_{4Lsw} = \frac{-k_{d5}}{b_{3L}}\left|S_{\psi_L}\right|^{0.5} sgn\left(S_{\psi_L}\right) - \frac{k_{d6}}{b_{3L}}\int sgn\left(S_{\psi_L}\right) \tag{27}$$

From Eqs. 19-27, constant parameters $k_1, k_2, k_3, k_4, k_5, k_6, k_{d1}, k_{d2}, k_{d3}, k_{d4}, k_{d5}, k_{d6}$ represent controllers and sliding surface gains. The coefficients are defined as follows: $a_{3L} = \frac{I_{zL}-I_{xL}}{I_{yL}}$, $a_{4L} = \frac{J_{rL}}{I_{yL}}$, $b_{2L} = \frac{l_L}{I_{yL}}$, $a_{5L} = \frac{I_{xL}-I_{yL}}{I_{zL}}$ and $b_{3L} = \frac{l_L}{I_{xL}}$. Moreover S_{θ_L} and S_{ψ_L} represent the sliding surfaces for θ_L and ψ_L loops. The corresponding error dynamics for θ_L and ψ_L loops are expressed as follows i.e., $e_{\theta_L} = \theta_L - \theta_{dL}$, $\dot{e_{\theta_L}} = \dot{\theta_L} - \dot{\theta_{dL}}$, $e_{\psi_L} = \psi_L - \psi_{dL}$, $\dot{e_{\psi_L}} = \dot{\psi_L} - \dot{\psi_{dL}}$.

Theorem 1: Consider the nonlinear system presented in Eq. 4-6, satisfying assumptions 1-3, then under the proposed controllers of Eq. 22-23, 24-25, states of the attitude dynamics will converge to the origin in finite time [32].

Proof of Theorem 1: The stability proof is only derived for ϕ_L loop only. Similar procedures can be adopted for the other two loops of attitude dynamics. Eq. 23 is modified as follows: $U_{2Lsw} = \frac{-k_{d1}}{b_{1L}}\left|S_{\phi_L}\right|^{0.5} sgn\left(S_{\phi_L}\right) + v_{\phi L}$; where the term $v_{\phi L}$ is calculated from the following expression: $\dot{v_{\phi L}} = \frac{k_{d2}}{b_{1L}} sgn\left(S_{\phi_L}\right)$. By combining the above terms with Eq. 21-22, $\dot{S_{\phi L}}$ is expressed as follows:

$$\dot{S_{\phi_L}} = \frac{-k_{d1}}{b_{1L}} \left|S_{\phi_L}\right|^{0.5} sgn\left(S_{\phi_L}\right) + v_{\phi L} - D_{\phi L}$$
$$\dot{v_{\phi L}} = -\frac{k_{d2}}{b_{1L}} sgn\left(S_{\phi_L}\right) \tag{28}$$

Let the Lyapunov function for ϕ loop dynamics is chosen as follows: $V_{\phi_L} = 2\tau_2\left|S_{\phi_L}\right| + 0.5v_{\phi L}^2 + 0.5\left(\tau_1\left|S_{\phi_L}\right|^{0.5} sgn\left(S_{\phi_L}\right) - v_{\phi L}\right)^2$. Where $\tau_1 = \frac{k_{d1}}{b_{1L}} and \tau_2 = \frac{k_{d2}}{b_{1L}}$. A new state vector is defined as follows: $\eta_{\phi L}^T = \left[\left|S_{\phi_L}\right|^{0.5} sgn\left(S_{\phi_L}\right)\ v_{\phi L}\right]$. Define matrix $P_{\phi L} = \begin{bmatrix} 4\tau_2 + \tau^2 & -\tau_1 \\ -\tau_1 & 2 \end{bmatrix}$ and then the Lyapunov function is expressed as follows: $V_{\phi_L} = \eta_{\phi L}^T P \eta_{\phi L}$. The time derivative of the Lyapunov function along (28) yields the following relation [32]:

$$\dot{V_{\phi_L}} = -\frac{1}{\left|S_{\phi_L}^{0.5}\right|} \eta_{\phi L}^T Q \eta_{\phi L} + \Delta_{4L} q_{\phi L}^T \eta_{\phi L} \tag{29}$$

Where the new matrices are represented as follows: $Q_{\phi L} = \frac{\tau_1}{2}\begin{pmatrix} 2\tau_2 + \tau_1^2 & -\tau_1 \\ -\tau_1 & 1 \end{pmatrix}$ and $q_{\phi L}^T = \left(2\tau_2 + \frac{1}{2}\tau_1^2 - \frac{1}{2}\tau_1\right)$. Applying the uncertainty bounds mentioned in Assumption 4, expression (29) is simplified as follows [32]:

$$\dot{V_{\phi L}} = -\frac{\tau_1}{2\left|S_{\phi L}^{0.5}\right|} \eta_{\phi L}^T \widetilde{Q_{\phi L}} \eta_{\phi L} \tag{30}$$

Where matrix $\widetilde{Q_{\phi L}} = \begin{pmatrix} 2\tau_2 + \tau_1^2 - \left(\frac{4\tau_2}{\tau_1} + \tau_1\right)\Delta_{4L} & -\tau_1 + 2\Delta_{4L} \\ -\tau_1 + 2\Delta_{4L} & 1 \end{pmatrix}$. Eq. 30 is negative definite only if $\widetilde{Q_{\phi L}} > 0$. If the gains satisfy the following criteria $\tau_1 > 2\Delta_{4L}$, $\tau_2 > \tau_1 \frac{5\Delta_{4L}\tau_1 + 4\Delta_{4L}^2}{2(\tau_1 - 2\Delta_{4L})}$, then $\tilde{Q} > 0$ and $\dot{V_{\phi_L}} < 0$.

Remark 1: The proof of finite time convergence property can be derived by using the procedures adopted in [32].

Altitude and position Control:

This section formulates the altitude and position control system for the leader UAV expressed in Eqs. 1-6. First the altitude control system is derived and then using the transformation matrix, the position controllers are formulated. With the desired altitude Z_{dL}, the sliding manifold is written as follows:

$$S_{Z_L} = k_7 e_{Z_L} + k_8 \dot{e}_{Z_L} \tag{31}$$

In Eq. 31, k_7 and k_8 represent the design constant. The error dynamics are defined as follows: i.e., $e_{Z_L} = Z_L - Z_{d_L}$, $\dot{e}_{Z_L} = \dot{Z}_L - \dot{Z}_{L_{d_L}}$. Taking the first-time derivative of Eq.32 yields the following expression:

$$\dot{S}_{Z_L} = k_7 \dot{e}_{Z_L} + k_8 \ddot{e}_{Z_L} \tag{32}$$

Eq. 32 and Eq. 3 are combined and expressed as follows:

$$\dot{S}_{Z_L} = k_7 \dot{e}_{Z_L} + k_8 \left[g - \cos\theta_L \cos\phi_L \frac{U_{1L}}{m_{QL}} - D_{ZL} - \ddot{Z}_{dL} \right] \tag{33}$$

Using super twisting sliding mode theory, the altitude controller is derived as follows:

$$U_{Z_L} = -\frac{k_7}{k_8} \dot{e}_{Z_L} + \ddot{Z}_{dL} - \frac{k_{d7}}{k_8} \left|S_{Z_L}\right|^{0.5} sgn\left(S_{Z_L}\right) - \frac{k_{d8}}{k_8} \int sgn\left(S_{Z_L}\right)$$

$$U_{1L} = \frac{m_{QL}}{\cos\theta_L \cos\phi_L} \left[g - \left(-\frac{k_7}{k_8} \dot{e}_{Z_L} + \ddot{Z}_{dL} - \frac{k_{d7}}{k_8} \left|S_{Z_L}\right|^{0.5} sgn\left(S_{Z_L}\right) - \frac{k_{d8}}{k_8} \int sgn\left(S_{Z_L}\right) \right) \right] \tag{34}$$

Here $U_{Z_L} = \ddot{Z}_L = g - (\cos\theta_L \cos\phi_L) \frac{U_{1L}}{m_{QL}}$ represents the virtual control law. The stability proof is derived based on the same concepts presented for ϕ loop. The robust terms of Eq. 34 are modified as follows: $U_{1Lsw} = \frac{-k_{d7}}{k_8} \left|S_{Z_L}\right|^{0.5} sgn\left(S_{Z_L}\right) + v_{Z_L}$; where the term v_{Z_L} is calculated from the following expression: $\dot{v}_{Z_L} = -\frac{k_{d8}}{k_8} sgn\left(S_{Z_L}\right)$. By combining the above terms with Eq. 33 and robust term of 34, $\dot{S}_{ZL}$ is expressed as follows:

$$\begin{aligned} \dot{S}_{Z_L} &= \frac{-k_{d7}}{k_8} \left|S_{Z_L}\right|^{0.5} sgn\left(S_{Z_L}\right) + v_{Z_L} - D_{ZL} \\ \dot{v}_{Z_L} &= -\frac{k_{d8}}{k_8} sgn\left(S_{Z_L}\right) \end{aligned} \tag{35}$$

Let the Lyapunov function for Z loop is chosen as follows: $V_{Z_L} = 2\tau_8 \left|S_{Z_L}\right| + 0.5 v_{Z_L}^2 + 0.5 \left(\tau_7 \left|S_{Z_L}\right|^{0.5} sgn\left(S_{Z_L}\right) - v_{Z_L}\right)^2$. Where $\tau_7 = \frac{k_{d7}}{k_8}$ and $\tau_8 = \frac{k_{d8}}{k_8}$. A new state vector is defined as follows: $\eta_{ZL}^T = \left[\left|S_{Z_L}\right|^{0.5} sgn\left(S_{Z_L}\right) \;\; v_{Z_L} \right]$. Define matrix $P_{ZL} = \begin{bmatrix} 4\tau_8 + \tau_7^2 & -\tau_7 \\ -\tau_7 & 2 \end{bmatrix}$ and then the Lyapunov function is expressed as follows: $V_{Z_L} = \eta_{ZL}^T P_{ZL} \eta_{ZL}$. The time derivative of the Lyapunov function along (35) yields the following relation [32]:

$$\dot{V}_{Z_L} = \eta_{ZL}^T Q_{ZL} \eta_{ZL} + \Delta_{3L} q_{ZL}^T \eta_{ZL} \tag{36}$$

Where the new matrices are represented as follows: $Q_{ZL} = \frac{\tau_7}{2}\begin{pmatrix} 2\tau_8 + \tau_7^2 & -\tau_7 \\ -\tau_7 & 1 \end{pmatrix}$ and $q_{ZL}^T = \left(2\tau_8 + \frac{1}{2}\tau_7^2 - \frac{1}{2}\tau_7\right)$. Applying the uncertainty bounds given in Assumption 4, expression (36) is simplified as follows [32]:

$$\dot{V_{ZL}} = -\frac{\tau_7}{2\left|S_{ZL}^{0.5}\right|}\eta_{ZL}^T\widetilde{Q_{ZL}}\eta_{ZL} \tag{37}$$

Where matrix $\widetilde{Q_{ZL}} = \begin{pmatrix} 2\tau_8 + \tau_7^2 - \left(\frac{4\tau_8}{\tau_7} + \tau_7\right)\Delta_{3L} & -\tau_7 + 2\Delta_{3L} \\ -\tau_7 + 2\Delta_{3L} & 1 \end{pmatrix}$. Eq. 37 is negative definite only if $\widetilde{Q_{ZL}} > 0$. If the gains satisfy the following criteria $\tau_7 > 2\Delta_{3L}$, $\tau_8 > \tau_7\frac{5\Delta_{3L}\tau_7 + 4\Delta_{3L}^2}{2(\tau_7 - 2\Delta_{3L})}$, then $\widetilde{Q_{ZL}} > 0$ and $\dot{V_{Z_L}} < 0$.

Now to derive the XY controllers, we assume the following:

$$U_{XL} = (\sin\psi_L \sin\phi_L + \cos\psi_L \sin\theta_L \cos\phi_L)\frac{U_{1L}}{m_{QL}}$$

$$U_{YL} = (-\cos\psi_L \sin\phi_L + \sin\psi_L \sin\theta_L \cos\phi_L)\frac{U_{1L}}{m_{QL}}$$

With these expressions, Eq 1 and 2 are re-written for leader UAV in the following form:

$$\ddot{X_L} = U_{XL} - D_{XL} \tag{38}$$

$$\ddot{Y_L} = U_{YL} - D_{YL} \tag{39}$$

Let the sliding manifolds for the position loops of leader UAV are expressed as follows:

$$\begin{aligned} S_{X_L} &= k_9 e_{X_L} + k_{10}\dot{e_{X_L}} \\ S_{Y_L} &= k_{11} e_{Y_L} + k_{12}\dot{e_{Y_L}} \end{aligned} \tag{40}$$

In Eq. 40 k_9, k_{10}, k_{11}, k_{12} are the design constants and the error dynamics are expressed as follows: $e_{X_L} = X_L - X_{dL}$, $\dot{e_{X_L}} = \dot{X_L} - \dot{X_{dL}}$, $e_{Y_L} = Y_L - Y_{dL}$, $\dot{e_{Y_L}} = \dot{Y_L} - \dot{Y_{dL}}$. By taking the first time derivative of Eq. 40, and combining it with Eq. 38 and 39 one acquires the following expressions:

$$\begin{aligned} \dot{S_{X_L}} &= k_9\dot{e_{X_L}} + k_{10}\left[U_{XL} - D_{XL} - \ddot{X_{dL}}\right] \\ \dot{S_{Y_L}} &= k_{11}\dot{e_{Y_L}} + k_{12}\left[U_{YL} - D_{YL} - \ddot{Y_{dL}}\right] \end{aligned} \tag{41}$$

From Eq. 41, the virtual controllers U_{XL} and U_{YL} are expressed as follows:

$$U_{XL} = \left(\ddot{X_{dL}} - \frac{k_9}{k_{10}} \dot{e_{X_L}} - \frac{k_{d9}}{k_{10}} \left|S_{X_L}\right|^{0.5} sgn\left(S_{X_L}\right) - \frac{k_{d10}}{k_{10}} \int sgn\left(S_{X_L}\right)\right)$$
$$U_{yL} = \left(\ddot{Y_{dL}} - \frac{k_{11}}{k_{12}} \dot{e_{Y_L}} - \frac{k_{d11}}{k_{12}} \left|S_{Y_L}\right|^{0.5} sgn\left(S_{Y_L}\right) - \frac{k_{d12}}{k_{12}} \int sgn\left(S_{Y_L}\right)\right) \quad (42)$$

The stability proof is derived based on the same concepts presented for Z loop. The robust terms of Eq. 42 are modified as follows: $U_{XLsw} = \frac{-k_{d9}}{k_{10}} \left|S_{X_L}\right|^{0.5} sgn\left(S_{X_L}\right) + v_{X_L}$; where the term v_{X_L} is calculated from the following expression: $\dot{v_{X_L}} = -\frac{k_{d10}}{k_{10}} sgn\left(S_{X_L}\right)$ and $U_{YLsw} = \frac{-k_{d11}}{k_{12}} \left|S_{Y_L}\right|^{0.5} sgn\left(S_{Y_L}\right) + v_{Y_L}$; where the term v_{Y_L} is calculated from the following expression: $\dot{v_{Y_L}} = -\frac{k_{d11}}{k_{12}} sgn\left(S_{Y_L}\right)$. By combining the above terms with Eq. 41 and 42, $\dot{S_{XL}}$ and $\dot{S_{YL}}$ are expressed as follows:

$$\dot{S_{X_L}} = \frac{-k_{d9}}{k_{10}} \left|S_{X_L}\right|^{0.5} sgn\left(S_{X_L}\right) + v_{X_L} - D_{XL}$$
$$\dot{v_{X_L}} = -\frac{k_{d10}}{k_{10}} sgn\left(S_{X_L}\right)$$
$$\dot{S_{YLL}} = \frac{-k_{d11}}{k_{12}} \left|S_{Y_L}\right|^{0.5} sgn\left(S_{Y_L}\right) + v_{Y_L} - D_{YL} \quad (43)$$
$$\dot{v_{Y_L}} = -\frac{k_{d12}}{k_{12}} sgn\left(S_{Y_L}\right)$$

Let the Lyapunov function for X loop dynamics is chosen as follows: $V_{X_L} = 2\tau_{10}\left|S_{X_L}\right| + 0.5 v_{X_L}^2 + 0.5\left(\tau_9 \left|S_{X_L}\right|^{0.5} sgn\left(S_{X_L}\right) - v_{X_L}\right)^2$, whereas for Y loop dynamics is the Lyapunov function is given as follows: $V_{Y_L} = 2\tau_{12}\left|S_{Y_L}\right| + 0.5 v_{Y_L}^2 + 0.5\left(\tau_{11} \left|S_{Y_L}\right|^{0.5} sgn\left(S_{Y_L}\right) - v_{Y_L}\right)^2$. Where $\tau_9 = \frac{k_{d9}}{k_{10}}$, $\tau_{10} = \frac{k_{d10}}{k_{10}}$, $\tau_{11} = \frac{k_{d11}}{k_{12}}$, $\tau_{12} = \frac{k_{d12}}{k_{12}}$.The following new state vectors are defined : $\eta_{XL}^T = \left[\left|S_{X_L}\right|^{0.5} sgn\left(S_{X_L}\right) \;\; v_{X_L}\right]$; $\eta_{YL}^T = \left[\left|S_{Y_L}\right|^{0.5} sgn\left(S_{Y_L}\right) \;\; v_{Y_L}\right]$. Define new matrices as follows: $P_{XL} = \begin{bmatrix} 4\tau_{10} + \tau_9^2 & -\tau_9 \\ -\tau_9 & 2 \end{bmatrix}$; $P_{YL} = \begin{bmatrix} 4\tau_{12} + \tau_{11}^2 & -\tau_{11} \\ -\tau_{11} & 2 \end{bmatrix}$ and then the Lyapunov functions are expressed as follows: $V_{X_L} = \zeta_1 \eta_{XL}^T P_{XL} \eta_{XL} + D_{XL}^T D_{XL}$; $V_{Y_L} = \zeta_2 \eta_{YL}^T P_{YL} \eta_{YL} + D_{YL}^T D_{YL}$. The time derivative of the Lyapunov functions along (43) yields the following relation [32]:

$$\begin{bmatrix} \dot{V_{X_L}} = -\zeta_1 \frac{1}{\left|S_{X_L}^{0.5}\right|} \eta_{XL}^T Q_{XL} \eta_{XL} + \zeta_1 D_{XL} q_{XL}^T \eta_{XL} + D_{XL}^T \dot{D_{XL}} \\ \dot{V_{Y_L}} = -\zeta_2 \frac{1}{\left|S_{Y_L}^{0.5}\right|} \eta_{YL}^T Q_{YL} \eta_{YL} + \zeta_2 D_{YL} q_{YL}^T \eta_{YL} + D_{YL}^T \dot{D_{YL}} \end{bmatrix} \tag{44}$$

Where: $Q_{XL} = \frac{\tau_9}{2}\begin{pmatrix} 2\tau_{10} + \tau_9^2 & -\tau_9 \\ -\tau_9 & 1 \end{pmatrix}$; $Q_{YL} = \frac{\tau_{11}}{2}\begin{pmatrix} 2\tau_{12} + \tau_{11}^2 & -\tau_{11} \\ -\tau_{11} & 1 \end{pmatrix}$and $q_{XL}^T = \left(2\tau_{10} + \frac{1}{2}\tau_9^2 \ \ -\frac{1}{2}\tau_9\right)$; $q_{YL}^T = \left(2\tau_{12} + \frac{1}{2}\tau_{11}^2 \ \ -\frac{1}{2}\tau_{11}\right)$. From Eq. 44, since D_{XL} and D_{YL} are scalar quantities so $D_{XL}^T = D_{XL}$ and $D_{YL}^T = D_{YL}$, then adaptive laws are derived as follows:

$$\begin{aligned} \dot{D_{XL}} &= -\zeta_1 q_{XL}^T \eta_{XL} \\ \dot{D_{YL}} &= -\zeta_2 q_{YL}^T \eta_{YL} \end{aligned} \tag{45}$$

Applying the uncertainty bounds given in Assumption 4 and by combining Eq. 44 with Eq.45, the simplified expressions of (44) are given as follows:[32]:

$$\begin{bmatrix} \dot{V_{XL}} = -\frac{\tau_9}{2\left|S_{XL}^{0.5}\right|} \eta_{XL}^T \widetilde{Q_{XL}} \eta_{XL} \\ \dot{V_{YL}} = -\frac{\tau_{11}}{2\left|S_{YL}^{0.5}\right|} \eta_{YL}^T \widetilde{Q_{YL}} \eta_{YL} \end{bmatrix} \tag{46}$$

Here the matrices are defined as follows:

$$\widetilde{Q_{XL}} = \begin{pmatrix} 2\tau_{10} + \tau_9^2 - \left(\frac{4\tau_{10}}{\tau_9} + \tau_9\right) \mathrm{E}\Delta_{1\mathrm{L}} & -\tau_9 + 2\mathrm{E}\Delta_{1\mathrm{L}} \\ -\tau_9 + 2\mathrm{E}\Delta_{1\mathrm{L}} & 1 \end{pmatrix}$$

and

$$\widetilde{\mathrm{Q_{YL}}} = \begin{pmatrix} 2\tau_{12} + \tau_{11}^2 - \left(\frac{4\tau_{12}}{\tau_{11}} + \tau_{11}\right) \mathrm{E}\Delta_{2\mathrm{L}} & -\tau_{11} + 2\mathrm{E}\Delta_{2\mathrm{L}} \\ -\tau_{11} + 2\mathrm{E}\Delta_{2\mathrm{L}} & 1 \end{pmatrix}$$

The expressions $\dot{V_{XL}}$ and $\dot{V_{YL}}$ are negative definite only if $\widetilde{Q_{XL}} > 0$ and $\widetilde{Q_{YL}} > 0$. If the gains satisfy the following criteria $\tau_9 > 2E\Delta_{1L}$, $\tau_{10} > \tau_9 \frac{5E\Delta_{1L}\tau_9 + 4E\Delta_{1L}^2}{2(\tau_9 - 2E\Delta_{1L})}$; $\tau_{11} > 2E\Delta_{2L}$, $\tau_{12} > \tau_{11} \frac{5E\Delta_{2L}\tau_{11} + 4E\Delta_{2L}^2}{2(\tau_{11} - 2E\Delta_{2L})}$, then $\widetilde{Q_{XL}} > 0$; $\widetilde{Q_{YL}} > 0$ and $\dot{V_{X_L}} < 0$; $\dot{V_{Y_L}} < 0$. Here the terms $E\Delta_{1L} = D_{XL_{estimated}} - D_{XL}$; $E\Delta_{2L} = D_{YL_{estimated}} - D_{YL}$ represent estimation error of the adaptive loops.

Remark 1: Discontinuous projection operator is used to implement the adaptive laws $\dot{D_{XL}}$, $\dot{D_{YL}}$. The projection operator is defined as follows:

$$projD_{(X,Y)L}(\star) = \begin{cases} 0 & if \quad D_{(X,Y)L} = D_{(X,Y)L_{max}} \quad ; \ \star > 0 \\ 0 & if \quad D_{(X,Y)L} = D_{(X,Y)L_{min}} \quad ; \ \star < 0 \\ \star & \qquad\qquad otherwise \end{cases} \tag{47}$$

In Eq. 45, ζ_1 and ζ_2 represent the adaptation gains. To generate reference trajectories for θ_{dL} and ϕ_{dL}, the virtual controllers U_{XL} and U_{YL} are expressed as follows:

$$\frac{U_{XL}m_{QL}}{U_{1L}} = \cos\psi_L \sin\theta_L \cos\phi_L + \sin\phi_L \sin\psi_L \tag{48}$$

$$\frac{U_{YL}m_{QL}}{U_{1L}} = \sin\psi_L \sin\theta_L \cos\phi_L - \cos\psi_L \sin\phi_L \tag{49}$$

Multiplying Eq-48 by $sin\psi$ and Eq.49 by $cos\psi$ and the deference of the resultant equations yields the following expression:

$$\frac{U_{XL}m_{QL}}{U_{1L}} \sin\psi - \frac{U_{YL}m_{QL}}{U_{1L}} \cos\psi = \sin\phi_{dL} \tag{50}$$

Eq. 50 is simplified to get the reference command for ϕ loop of the leader UAV as follows:

$$\phi_{dL} = \sin^{-1}\left[\frac{U_{XL}m_{QL}}{U_{1L}} \sin\psi - \frac{U_{YL}m_{QL}}{U_{1L}} \cos\psi\right] \tag{51}$$

Multiplying Eq-48 by $cos\psi$ and Eq.49 by $sin\psi$ and the summation of the resultant equations yields the following expression:

$$\frac{U_{XL}m_{QL}}{U_{1L}} \cos\psi + \frac{U_{YL}m_{QL}}{U_{1L}} \sin\psi = \sin\theta_{dL} \cos\phi_{dL} \tag{52}$$

Squaring Eq. 50 on both hand sides and equating $\sin^2\phi_{dL} = 1 - \cos^2\phi_{dL}$, the expression is written in terms of $\cos\phi_{dL}$ and given as follows:

$$\cos\phi_{dL} = \sqrt{1 - \left[\frac{U_{XL}m_{QL}}{U_{1L}} \sin\psi - \frac{U_{YL}m_{QL}}{U_{1L}} \cos\psi\right]^2} \tag{53}$$

Now form Eqs. 51 and 52, reference command for θ_{dL} is expressed as follows:

$$\theta_{dL} = \sin^{-1}\left[\frac{\frac{U_{XL}m_{QL}}{U_{1L}} \cos\psi + \frac{U_{YL}m_{QL}}{U_{1L}} \sin\psi}{\sqrt{1 - \left[\frac{U_{XL}m_{QL}}{U_{1L}} \sin\psi - \frac{U_{YL}m_{QL}}{U_{1L}} \cos\psi\right]^2}}\right] \tag{54}$$

3.2 LEADER FOLLOWER FORMATION CONTROL

Before discussing the trajectory controllers for the follower UAVs, it is necessary to derive the formation controller which will generate the desired trajectory for the follower UAVs. Let the

following sliding surface is defined for formation controller:

$$S_{\chi j} = \chi j + \tau \int \chi j \tag{55}$$

Where τ represents gain matrix of the sliding surface. By taking time derivative of Eq. 55 and combining it with Eq. 14, one obtains the following expression:

$$\dot{S_{\chi J}} = F(\chi j) + G(\chi j) vj + \tau \chi j \tag{56}$$

For formation control, the desired longitudinal and lateral velocities of the follower UAVs are calculated as follows:

$$vj_{eq} = G(\chi j)^{-1}[-F(\chi j) - \tau \chi j] \tag{57}$$

$$vj_{sw} = -\eta_1 \left|S_{\chi j}\right|^{0.5} sgn\left(S_{\chi j}\right) - \eta_2 \int sgn\left(S_{\chi j}\right) \tag{58}$$

For stability proof, same procedures as adopted for XYZ loops are applied here.

3.3 FOLLOWER UAVs CONTROL FORMULATION

In this section we briefly explain the trajectory control of follower UAVs. As mentioned above, the reference position trajectories are generated using Eq. 18, and governed by the formation controller of Eq. 57. Thus, by defining the attitude, altitude and position errors for the follower UAVs, the rest of the analysis used for the derivation of the subject controllers is the same as leader UAV. For simplicity, here the final control laws are included: let the attitude sliding manifolds are defined as follows:

$$\begin{aligned} S_{\phi j} &= k_{1j} e_{\phi_j} + k_{2j}\, \dot{e_{\phi_j}} \\ S_{\theta j} &= k_{3j} e_{\theta_j} + k_{4j}\, \dot{e_{\theta_j}} \\ S_{\psi j} &= k_{5j} e_{\psi_j} + k_{6j}\, \dot{e_{\psi_j}} \end{aligned} \tag{59}$$

Where $j = [F_1, F_2]$ and F_1 and F_2 represent follower 1 and follower 2 UAVs respectively. Also k_{1j}, k_{2j}, k_{3j}, k_{4j}, k_{5j}, k_{6j} represent the constants of sliding surfaces for follower UAVs. The respective errors are defined as follows: $e_{\phi_j} = \phi_j - \phi_{dj}$; $e_{\theta_j} = \theta_j - \theta_{dj}$; $e_{\psi_j} = \psi_j - \psi_{dj}$. Similarly position and altitude sliding manifolds for follower 1 and 2 are given as follows:

$$\begin{aligned} S_{Zj} &= k_{7j} e_{Zj} + k_{8j} \dot{e_{Z_j}} \\ S_{Xj} &= k_{9j} e_{Xj} + k_{10j} \dot{e_{X_j}} \\ S_{Yj} &= k_{11j} e_{Yj} + k_{12j} \dot{e_{Y_j}} \end{aligned} \tag{60}$$

Where $k_{7j}, k_{8j}, k_{9j}, k_{10j}, k_{11j}, k_{12j}$ represent the constants of sliding surfaces for follower UAVs. The respective errors are defined as follows: $e_{Z_j} = Z_j - Z_{dj}$; $e_{X_j} = X_j - X_{dj}$; $e_{Y_j} = Y_j -$

Y_{dj}. Now following the same procedures, the attitude, altitude and position controllers for follower UAVs are formulated as follows:

$$U_{2jeq} = \frac{1}{b_{1j}}\left(\frac{-k_{1j}}{k_{2j}}\dot{e_{\phi_j}} - a_{1j}\theta_j\dot{\psi}_j + a_{2j}\dot{\theta}_j\Omega_{rj} + \ddot{\phi_{dj}}\right) \tag{61}$$

$$U_{2jsw} = \frac{-k_{d1j}}{b_{1j}}\left|S_{\phi_j}\right|^{0.5} sgn\left(S_{\phi_j}\right) - \frac{k_{d2j}}{b_{1j}}\int sgn\left(S_{\phi_j}\right) \tag{62}$$

$$U_{3jeq} = \frac{1}{b_{2j}}\left(\frac{-k_{3j}}{k_{4j}}\dot{e_{\theta_j}} - a_{3j}\phi_j\dot{\psi}_j + a_{4j}\dot{\phi}_j\Omega_{rj} + \ddot{\theta_{dj}}\right) \tag{63}$$

$$U_{3jsw} = \frac{-k_{d3j}}{b_{2j}}\left|S_{\theta_j}\right|^{0.5} sgn\left(S_{\theta_j}\right) - \frac{k_{d4j}}{b_{2j}}\int sgn\left(S_{\theta_j}\right) \tag{64}$$

$$U_{4jeq} = \frac{1}{b_{3j}}\left(\frac{-k_{5j}}{k_{6j}}\dot{e_{\psi_j}} - a_{5j}\phi_j\dot{\theta}_j + \ddot{\psi_{dj}}\right) \tag{65}$$

$$U_{4jsw} = \frac{-k_{d5j}}{b_{3j}}\left|S_{\psi_j}\right|^{0.5} sgn\left(S_{\psi_j}\right) - \frac{k_{d6j}}{b_{3j}}\int sgn\left(S_{\psi_j}\right) \tag{66}$$

$$\begin{aligned} U_{1j} = \frac{m_{Qj}}{\cos\theta_j\cos\phi_j}\Bigg[-\Bigg(-\frac{k_7 j}{k_{8j}}\dot{e_{Z_j}} + \ddot{Z_{dj}} - \frac{k_{d7j}}{k_{8j}}\left|S_{Z_j}\right|^{0.5} sgn\left(S_{Z_j}\right) \\ - \frac{k_{d8j}}{k_{8j}}\int sgn\left(S_{Z_j}\right)\Bigg)\Bigg] \end{aligned} \tag{67}$$

$$\begin{aligned} U_{Xj} &= \left(\ddot{X_{dj}} - \frac{k_{9j}}{k_{10j}}\dot{e_{X_j}} - \frac{k_{d9j}}{k_{10j}}\left|S_{X_j}\right|^{0.5} sgn\left(S_{X_j}\right) - \frac{k_{d10j}}{k_{10j}}\int sgn\left(S_{X_j}\right)\right) \\ U_{yj} &= \left(\ddot{Y_{dj}} - \frac{k_{11j}}{k_{12j}}\dot{e_{Y_j}} - \frac{k_{d11j}}{k_{12}j}\left|S_{Y_j}\right|^{0.5} sgn\left(S_{Y_j}\right) - \frac{k_{d12j}}{k_{12}j}\int sgn\left(S_{Y_j}\right)\right) \end{aligned} \tag{68}$$

$$\begin{aligned} \dot{D_{X_j}} &= -\zeta_1 j S_{X_j} \\ \dot{D_{Y_j}} &= -\zeta_2 j S_{Y_j} \end{aligned} \tag{69}$$

The reference commands for θ_{dj} and ϕ_{dj} are derived using the same procedures given in Eq. 48-54.

CHAPTER 4: RESULTS AND DISCUSSIONS

In this section, the proposed ASTSMC controller is tested numerically for the system of multiple quad-rotors shown in Fig. 2. The parameters of the leader and follower UAVs are identical and given in Table 1. The control parameters of leader and follower UAVs are given in Table 2 and 3. Since the UAVs are identical, thus leader and follower UAVs use the same control parameters. The parameters for formation control loops are chosen as follows: $\tau_{F1} = \tau_{F2} = \begin{bmatrix} 1.5 \\ 1.5 \\ 0.5 \end{bmatrix}$, $\eta_{1F1} = \eta_{1F2} = \begin{bmatrix} 0.1 \\ 0.1 \\ 0.075 \end{bmatrix}$, $\eta_{2F1} = \eta_{2F2} = \begin{bmatrix} 0.05 \\ 0.05 \\ 0.02 \end{bmatrix}$. For the leader UAV, the reference position and altitude commands are set as follows: $X_L = \sin t$, $Y_L = \cos t$ and $Z_L = t$. Figure 3 shows the applied acceleration disturbance on X and Y dynamics of the leader and follower UAVs. It is assumed that same type of disturbance acceleration is applied for all UAVs. Furthermore, the disturbance acceleration has no effect on the Z dynamics of UAV. Moreover the following parametric uncertainties are applied: $a_{1L} = 2.5a_{1L}$; $a_{1j} = 2.5a_{1j}$; $a_{2L} = 2.5a_{2L}$; $a_{2j} = 2.5a_{2j}$; $a_{3L} = 2.5a_{3L}$; $a_{3j} = 2.5a_{3j}$; $a_{4L} = 2.5a_{4L}$; $a_{4j} = 2.5a_{4j}$; $a_{5L} = 2.5a_{5L}$; $a_{5j} = 2.5a_{5j}$; $b_{1L} = 1.75b_{1L}$; $b_{1j} = 1.75b_{1j}$; $b_{2L} = 1.75b_{2L}$; $b_{2j} = 1.75b_{2j}$; $b_{3L} = 1.75b_{3L}$; $b_{3j} = 1.75b_{3j}$.

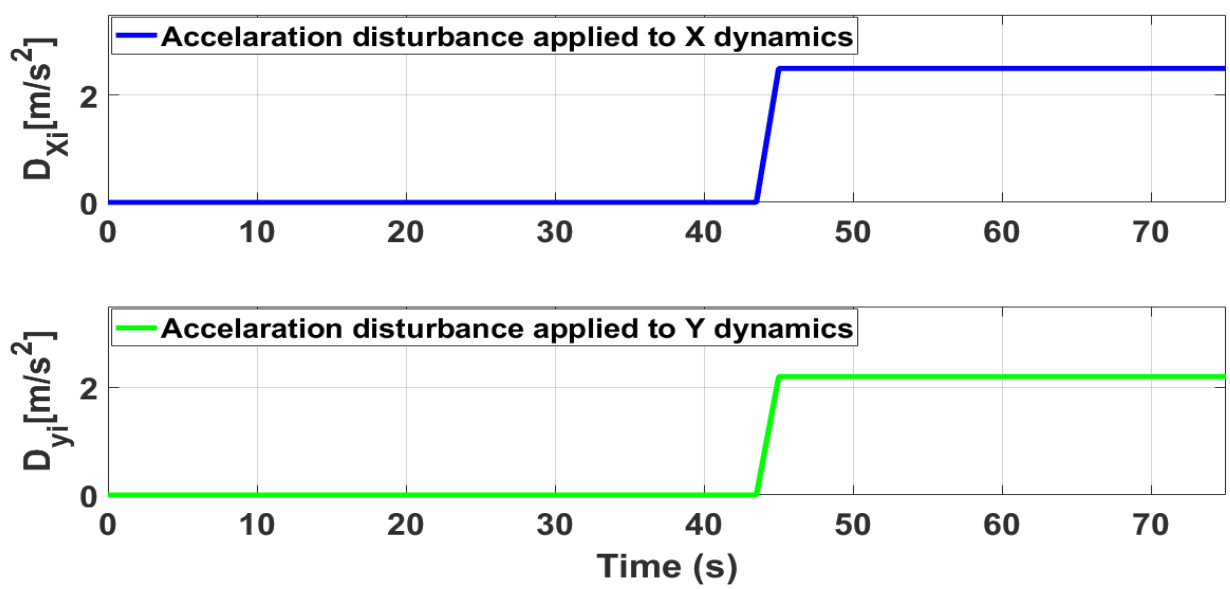

Figure 3: Applied acceleration type disturbance in X and Y dynamics

Table 1: Leader-followers UAV parameters.

Symbol	Value	Unit
$m_{QL} = m_{F1} = m_{F1}$	0.65	Kg
$l_L = l_{F1} = l_{F2}$	0.23	m
$J_{rL} = J_{F1} = J_{F2}$	$6.5 * 10^{-5}$	$kg.m^2$
$I_{xL} = I_{xF1} = I_{xF2}$	$7.5 * 10^{-3}$	Ns^2rad^{-1}
$I_{yL} = I_{yF1} = I_{yF2}$	$7.5 * 10^{-3}$	Ns^2rad^{-1}
$I_{zL} = I_{zF1} = I_{zF2}$	$1.3 * 10^{-2}$	Ns^2rad^{-1}

Table 2: Leader UAV control parameters for attitude, altitude and position loops

Parameter	Value	Parameter	Value
k_1	200	k_2	1
k_{d1}	70	k_{d2}	15
k_3	200	k_4	1
k_{d3}	50	k_{d4}	10
k_5	95	k_6	1
k_{d5}	4.6	k_{d6}	0.5
k_7	97	k_8	1
k_{d7}	300	k_{d8}	1.5
k_9	60	k_{10}	1000
k_{d9}	2.5	k_{d10}	180
k_{11}	60	k_{12}	1000
k_{d11}	2.5	k_{d12}	5
ζ_1	1.5	ζ_2	2.5

Table 3: Follower UAVs control parameters for attitude, altitude and position loops.

Parameter	Value	Parameter	Value
k_{1j}	200	k_{2j}	1
k_{d1j}	70	k_{d2j}	15
k_{3j}	200	k_{4j}	1
k_{d3j}	50	k_{d4j}	10
k_{5j}	95	k_{6j}	1
k_{d5j}	4.6	k_{d6j}	0.5
k_{7j}	97	k_{8j}	1
k_{d7j}	300	k_{d8j}	1.5
k_{9j}	60	k_{10j}	1000
k_{d9j}	2.5	k_{d10j}	180
k_{11j}	60	k_{12j}	1000
k_{d11j}	2.5	k_{d12j}	5
ζ_{1j}	1.5	ζ_{2j}	2.5

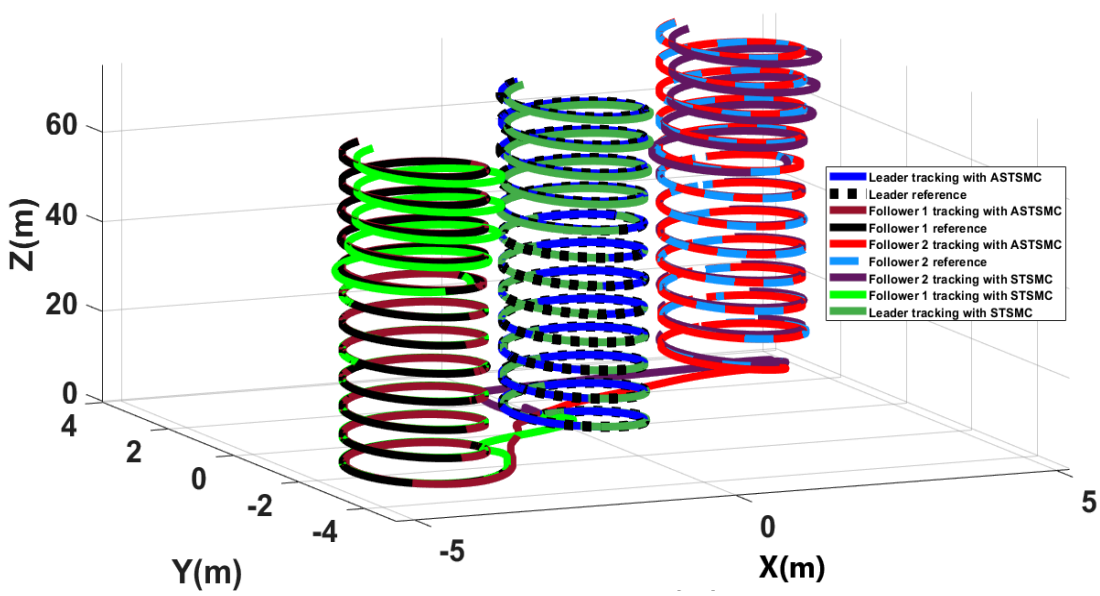

Figure 4: XYZ trajectory tracking comparison under wind disturbance

Figure. 4 shows the trajectory tracking simulations of leader follower UAVs in presence of applied disturbance of Figure.3. From the presented results, it is concluded that in presence of

disturbances, ASTSMC controllers ensure robust behavior, while the fixed gain STSMC controllers exhibit steady state errors in the X and Y tracking responses of the leader and follower UAVs.

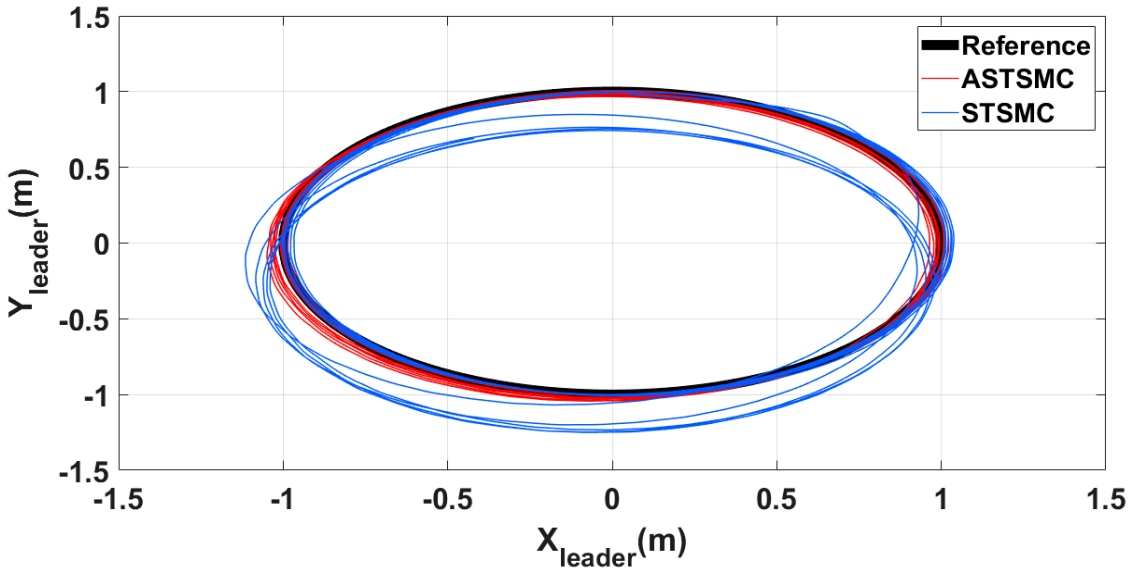

Figure 5: XY leader trajectory tracking comparison under wind disturbance

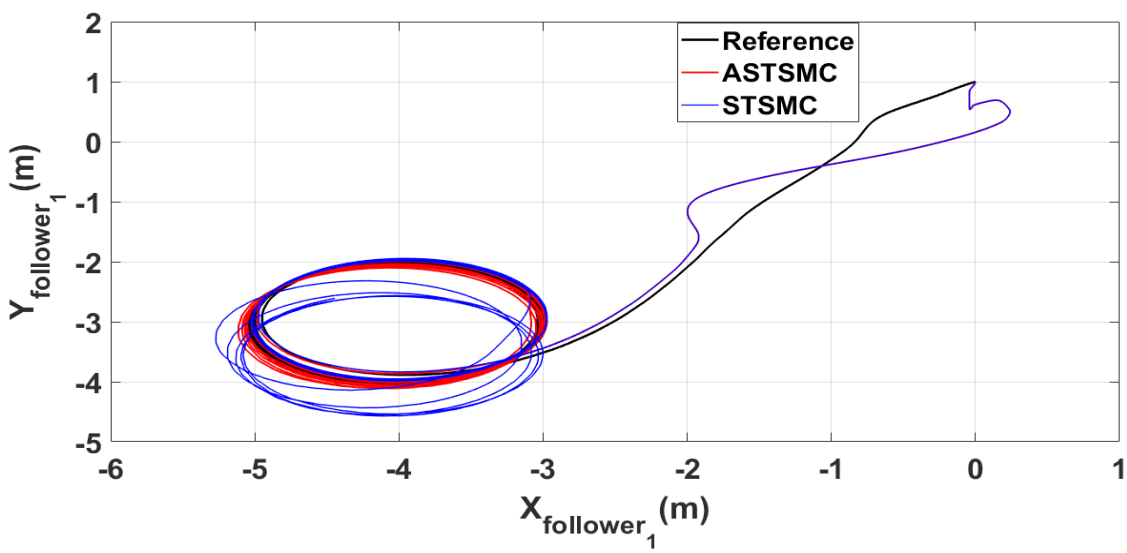

Figure 6: XY follower 1 trajectory tracking comparison under wind disturbance

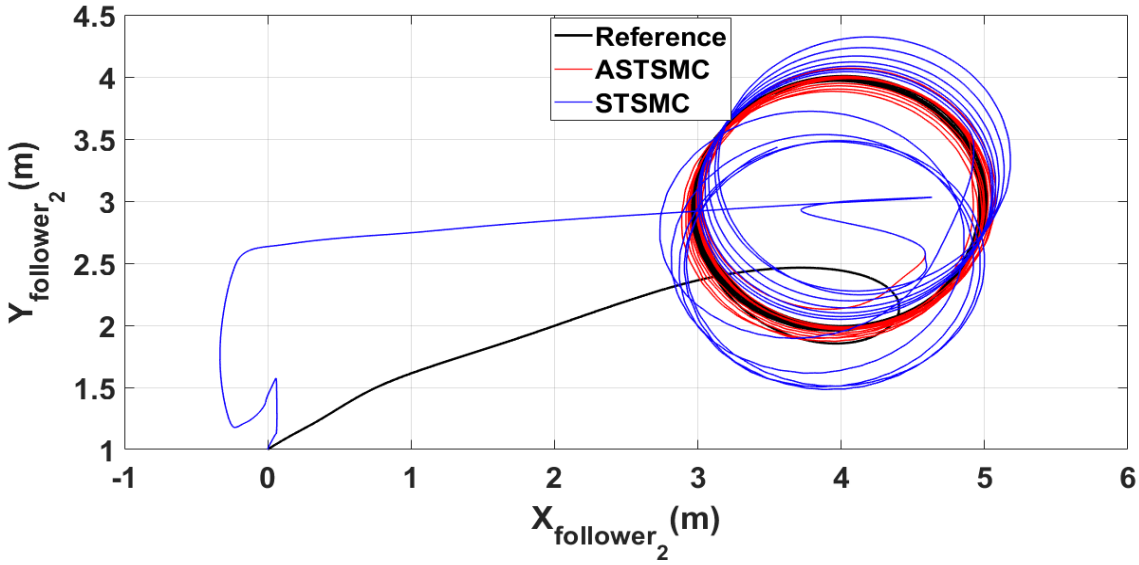

Figure 7: *XY* follower 2 trajectory tracking comparison under wind disturbance

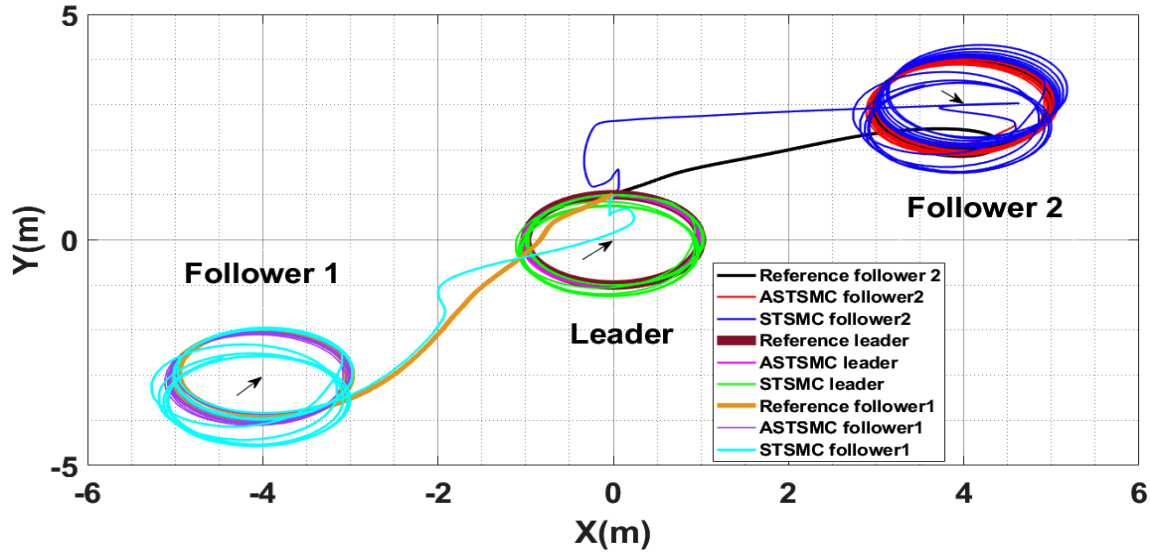

Figure 8: *XY* Leader-followers trajectory tracking comparison under wind disturbance

In order to have a clear picture of the trajectory deviations under wind disturbance, Fig. 5, 6, 7 and 8 show the trajectory tracking comparisons in XY plane for leader, follower 1 and follower 2 UAVs respectively. From the presented results it is concluded that minimum deviations are observed in the trajectory tracking for all UAVs with ASTSMC controllers, while with fixed gain STSMC controllers all UAVs show significant drift from the reference trajectories in XY plane. Figure 8 shows the combined trajectories of leader followers UAVs with ASTSMC and fixed gain STSMC controllers in XY plane. From the presented results, it is obvious that the proposed ASTSMC controllers ensure robust formation control between the leader and followers UAVs, while with fixed gain STSMC controllers, all UAVs show drift in their trajectories.

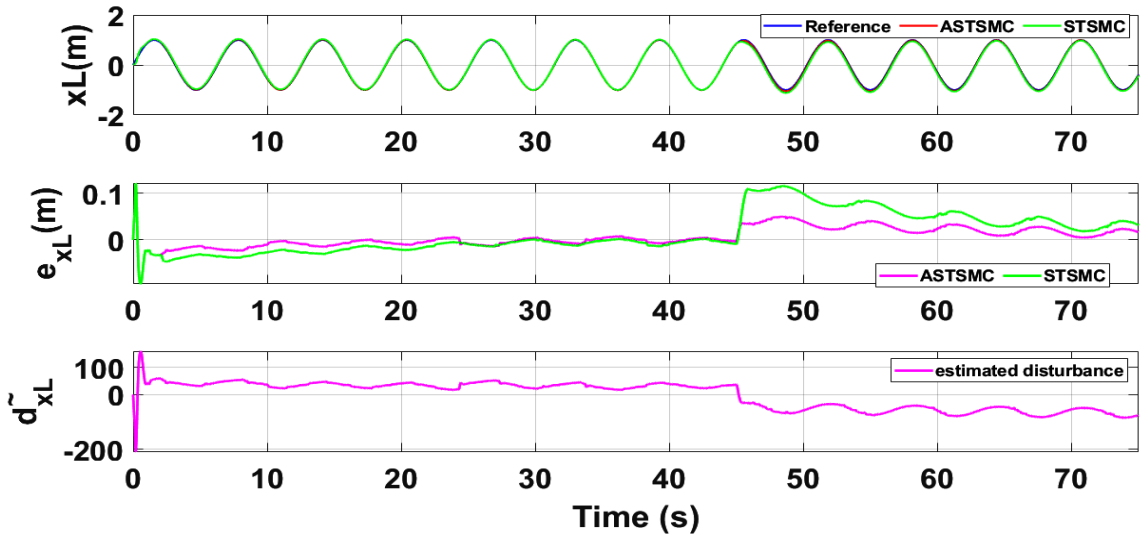

Figure 9: X_{leader} tracking comparison under wind disturbance

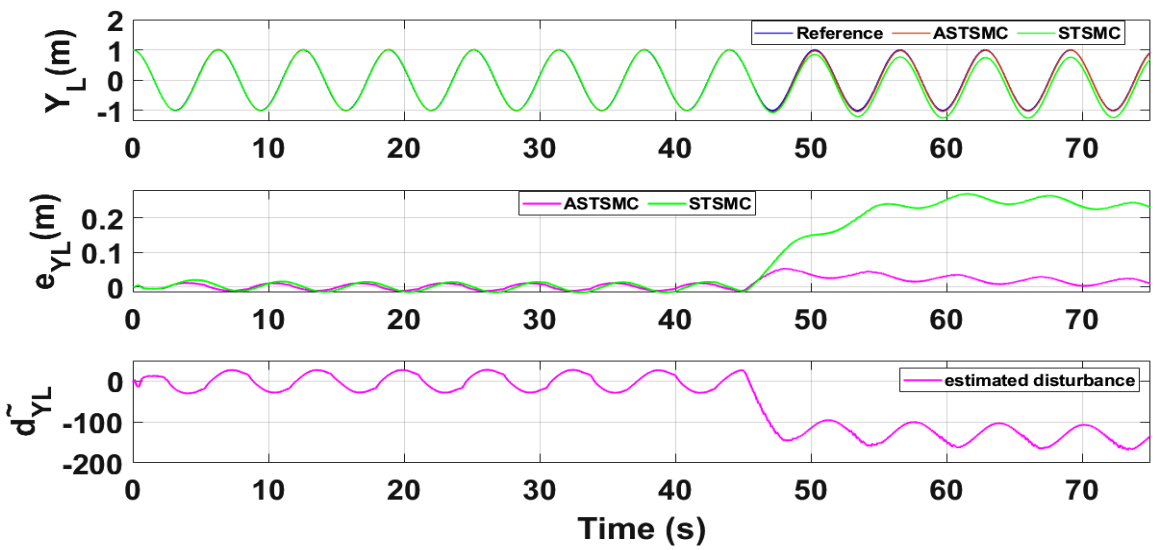

Figure 10: Y_{leader} tracking comparison under wind disturbance

In order to compare the trajectory tracking performance of the leader follower UAVs quantitatively, the X and Y trajectories are individually plotted against time and the results are presented in Fig. 9 and 10 for the leader UAV. From Fig.9, and at time $t = 45sec$, the e_{XL} tracking error is 0.1 m with fixed gain STSMC controller while with ASTSMC controller, the measured error e_{XL} is 0.05. ASTSMC ensures lowest error due the adaptive disturbance compensation term D_{XL} and from the presented results of Fig.9, it is obvious that at time $t = 45s$, the adaptive term D_{XL} adds appropriate compensation to cancel the disturbance and it switches from 50 to -100. Similarly, from Fig.10, e_{YL} is measured 0.28m and 0.05m with fixed gain STSMC and ASTSMC controllers respectively. ASTSMC controller offers lowest error due to the adaptive estimator term

D_{YL}. From the presented results of Fig.10, it is obvious that at time $t = 45s$, the adaptive term D_{YL} adds appropriate compensation to cancel the disturbance and it switches from 0 to -150. Similarly for followers UAV, the X and Y tracking responses are plotted against simulation time and the results are shown in Fig. 11, 12, 13 and 14. From the presented results and at time $t = 45s$, the measured error signals with fixed gain STSMC controller are as follows: $e_{X_{F1}} = 0.2m$, $e_{Y_{F1}} = 0.3m$, $e_{X_{F2}} = 0.2m$, $e_{Y_{F1}} = 0.5m$, while with ASTSMC controllers, the errors are measured as follows: $e_{X_{F1}} = 0.1m$, $e_{Y_{F1}} = 0.1m$, $e_{X_{F2}} = 0.05m$, $e_{Y_{F1}} = 0.05m$. From the presented results of Fig.11, 12, 13 and 14, it is obvious that at time $t = 45s$, the adaptive terms $D_{X_{F1}}$, $D_{Y_{F1}}$, $D_{X_{F2}}$, $D_{Y_{F2}}$ add appropriate compensation to cancel the disturbances.

Fig. 15 and 16 show θ and ϕ tracking responses for leader and follower UAVs with both fixed gain STSMC and ASTSMC controllers respectively. From the presented results and at time $t = 45s$, it is evident that the proposed ASTSMC controllers generate appropriate reference commands for both θ and ϕ loops of leader and follower UAVs. In order to have better understanding of the above claim, Fig. 17 shows the difference of the generated reference θ and ϕ commands with ASTSMC and fixed gain STSMC controllers. From the presented results, it is obvious that at time $t = 45s$, the proposed ASTSMC controllers generate appropriate reference commands for both θ and ϕ loops of leader and follower UAVs.

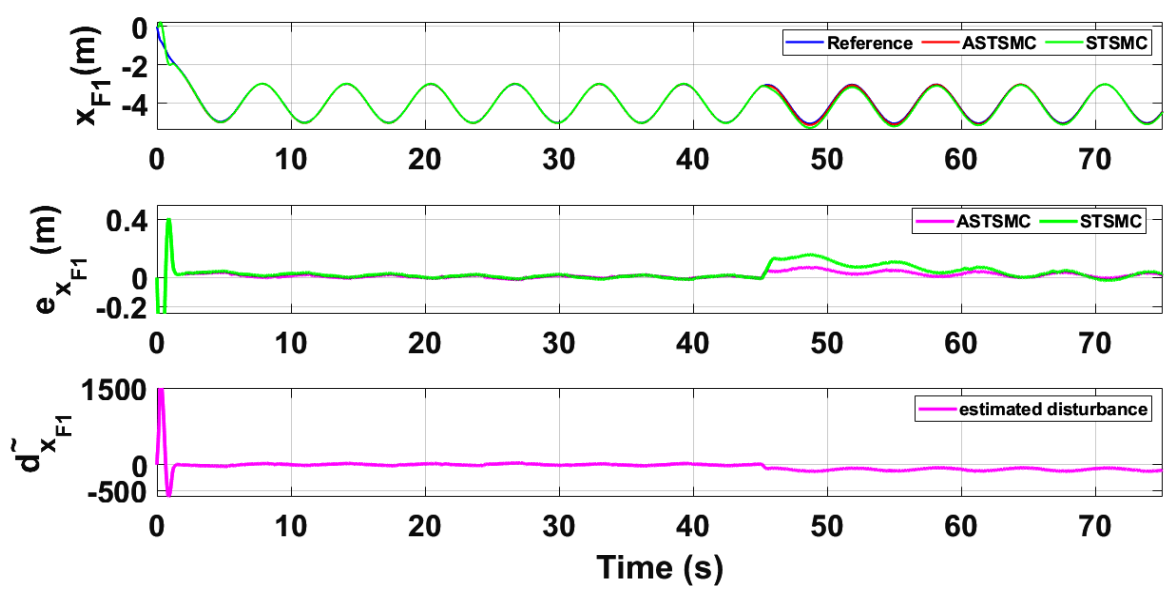

Figure 11: X_{F1} tracking comparison under wind disturbance

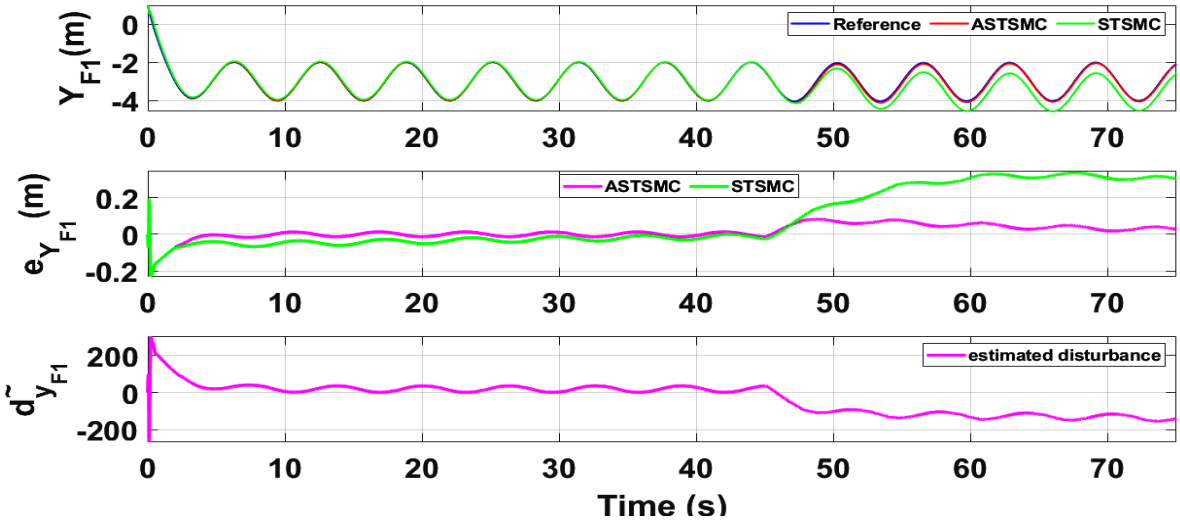

Figure 12: Y_{F1} tracking comparison under wind disturbance

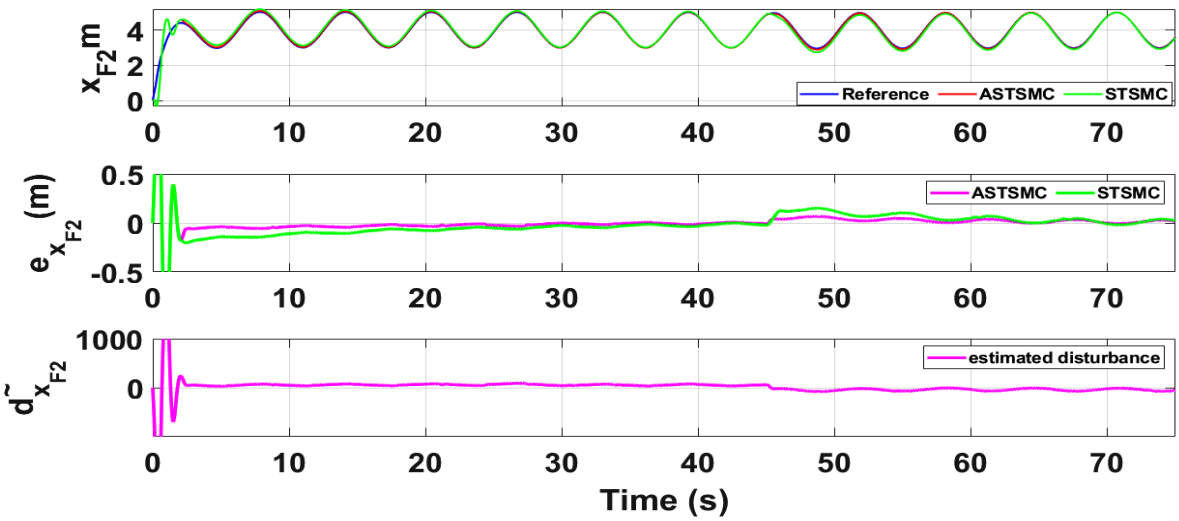

Figure 13: X_{F2} tracking comparison under wind disturbance

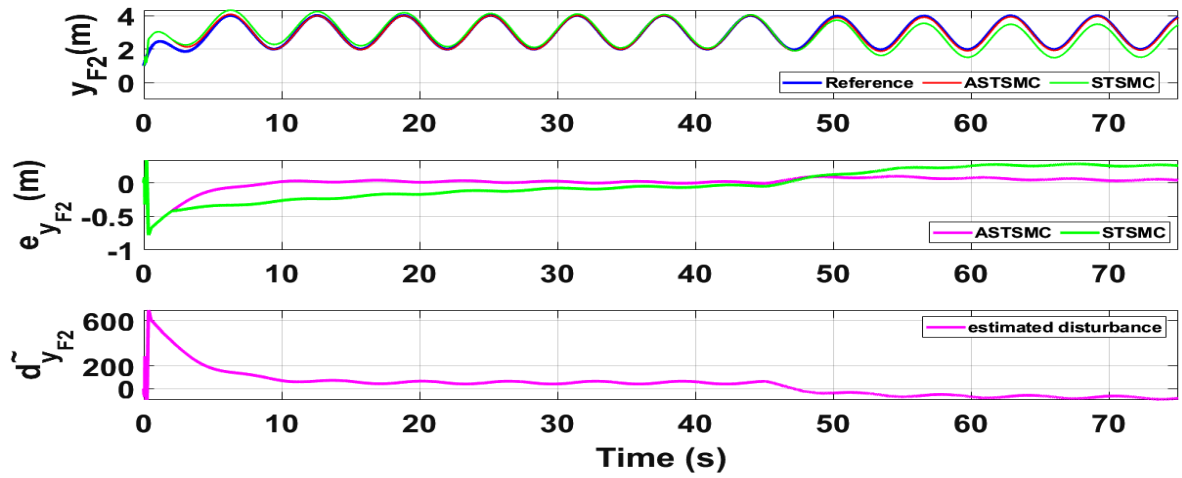

Figure 14: Y_{F2} tracking comparison under wind disturbance

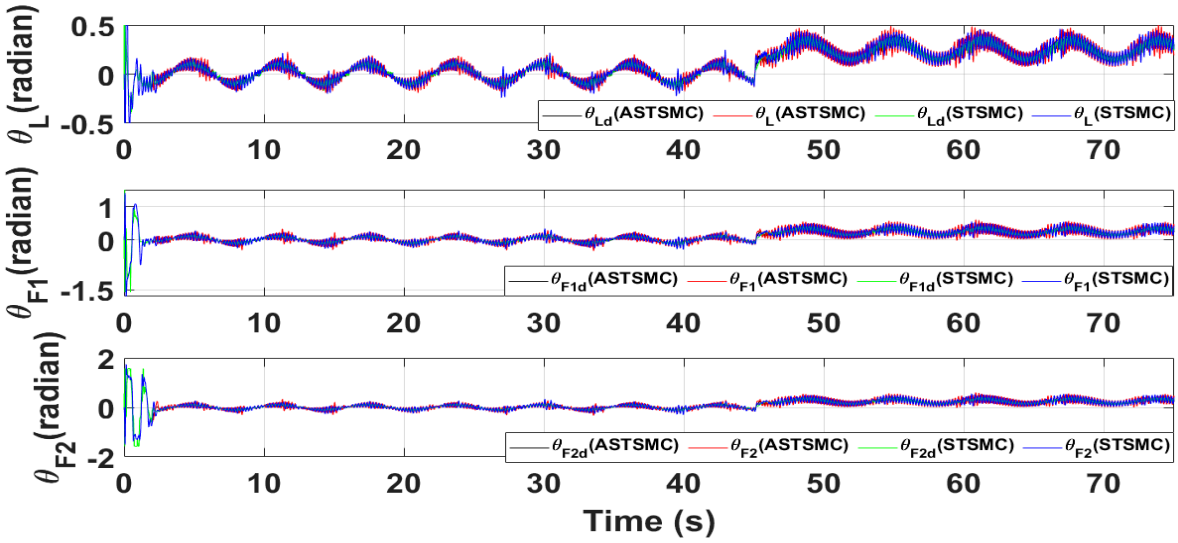

Figure 15: θ tracking comparison under wind disturbance

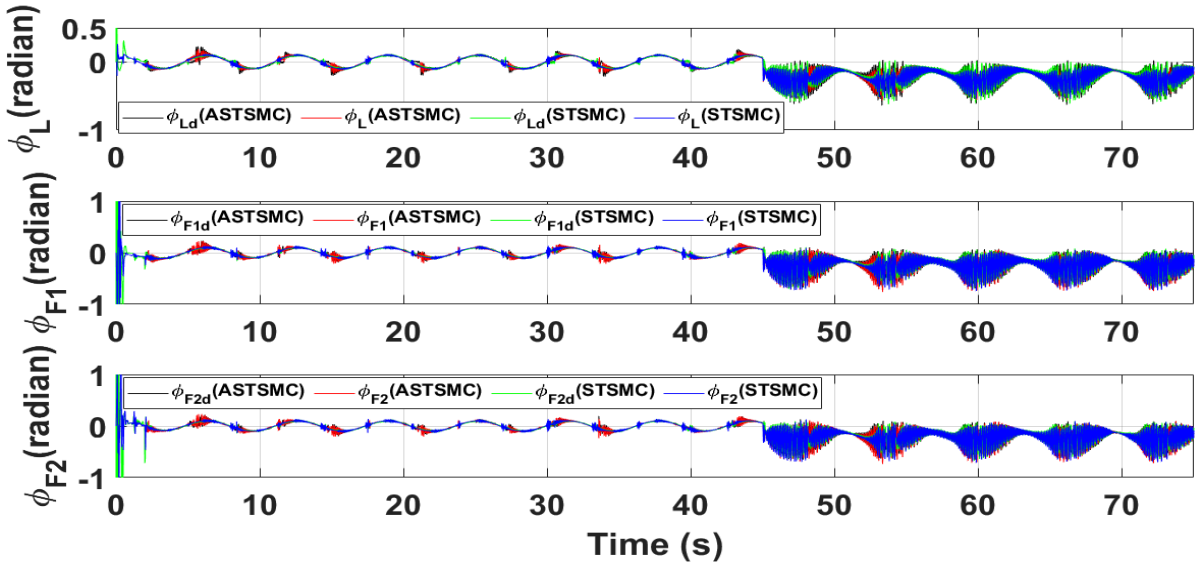

Figure 16: ϕ tracking comparison under wind disturbance

Fig. 18 and 19 show Z and ψ loops tracking responses for leader and follower UAVs. Since no disturbances are applied on both these loops, thus the tracking responses under fixed gain STSMC and ASTSMC controllers are comparable. Finally, Fig. 20 shows the robustness of the formation controllers for tracking the respective reference commands i.e., the distance between the leader and the followers in X, Y plane. From the presented results it is obvious that apart from the transient error, the formation controllers accurately maintain the desired distance between the leader- follower 1 and leader-follower 2 UAVs.

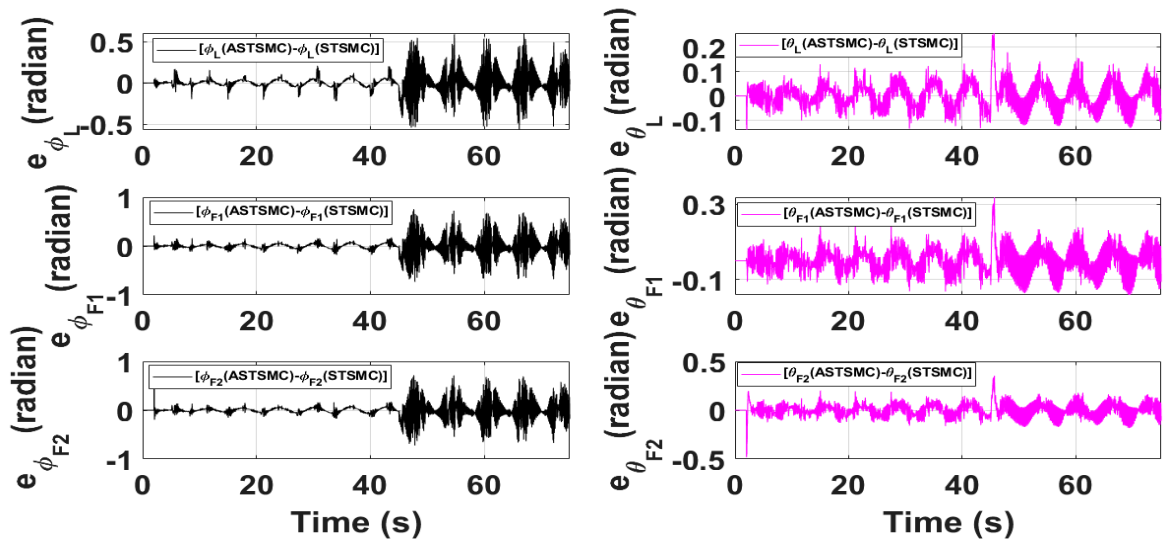

Figure 17: Difference between desired θ, ϕ with ASTSMC and STSMC controllers

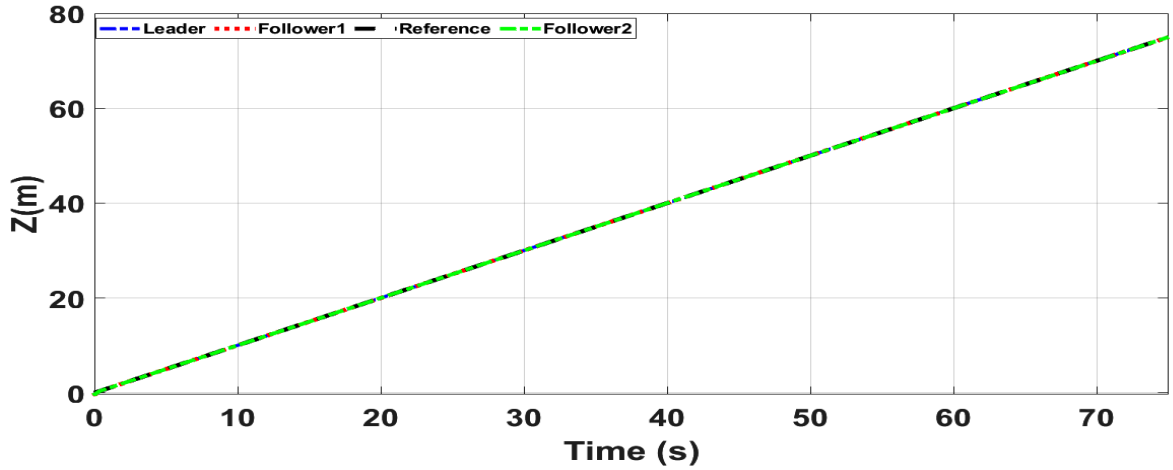

Figure 18: *z* tracking

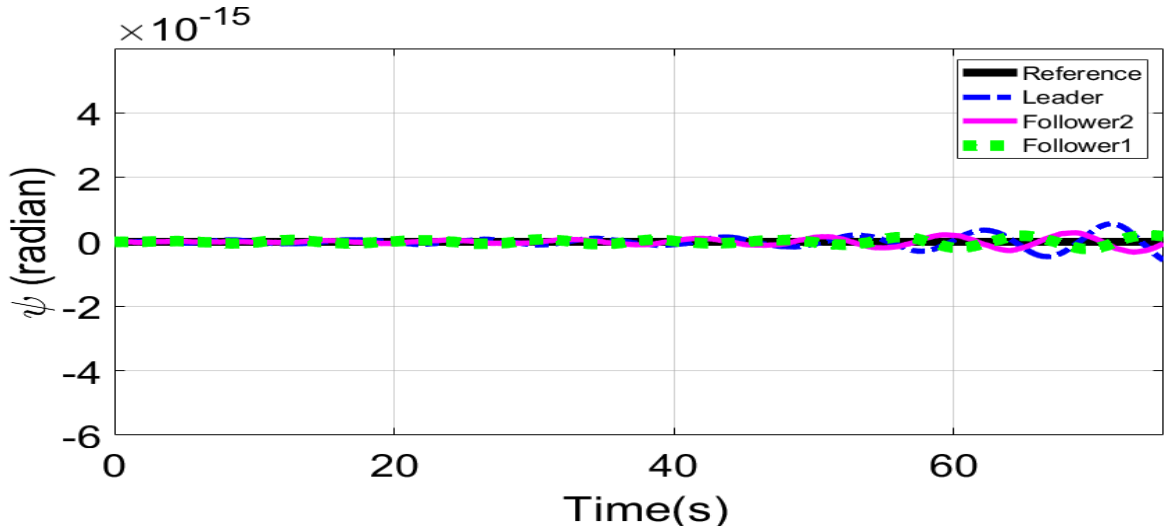

Figure 19: ψ tracking

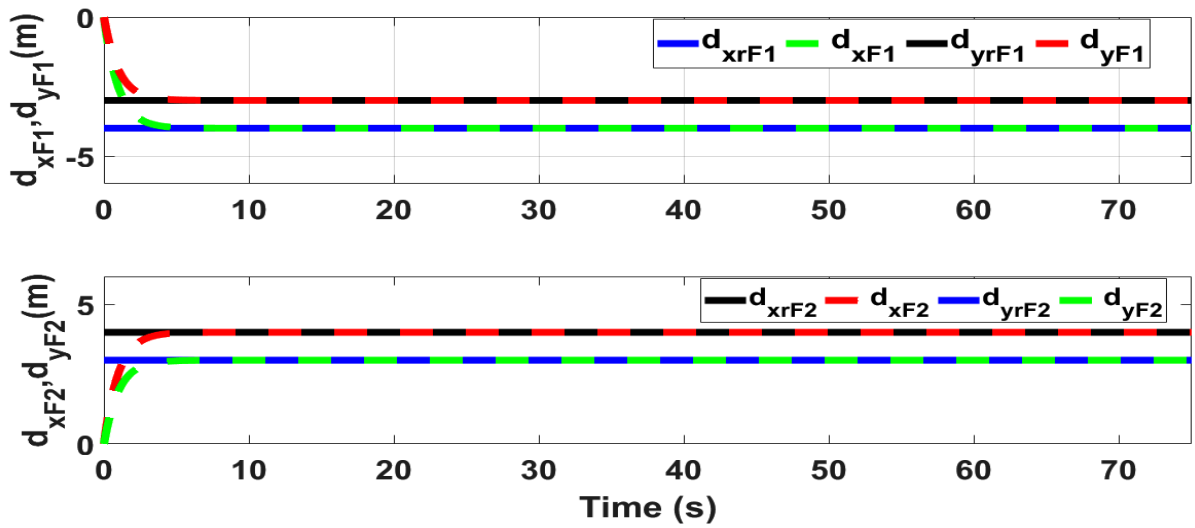

Figure 20: Formation controller tracking

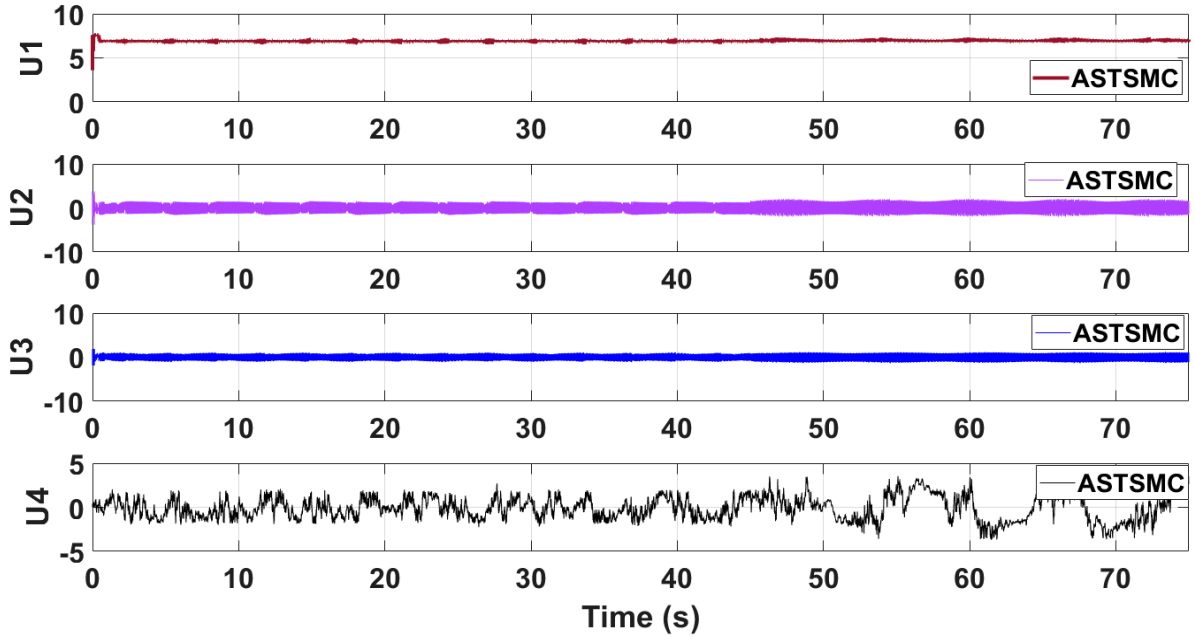

Figure 21: Control inputs using proposed control scheme

Figure 21 shows the simulation results of the control inputs using the proposed control schemes. Since the attitude loops are not adaptive and gains are fixed so the control signals chatters, however the control inputs are feasible for practical implementations and well bounded. Moreover, the virtual XY control outputs of the proposed control schemes offer vert low chattering (Fig. 15-16) In future work, gains of the proposed control schemes will be tuned online to overcome the chattering phenomena.

CHAPTER 5: CONCLUSIONS

This paper proposes adaptive super twisting sliding mode trajectory and formation controllers for multiple UAVs flying the leader follower configuration. Acceleration type disturbances are applied to X and Y dynamics of leader and follower UAVs. The formation control of UAVs is tested with the proposed ASTSMC and fixed gain STSMC controllers. The robust performance of the proposed control is verified from the following measured errors of the leader and follower UAVs. For leader UAV, e_{XL}= 0.05m, e_{YL}= 0.05m with ASTSMC control while with the fixed gain STSMC controller, the measured errors are as follows: e_{XL}= 0.1m, e_{YL}= 0.25m. Similarly, for follower UAVs, e_{XF1}= 0.09m, e_{YF1}= 0.05m, e_{XF2}= 0.09m, e_{YF2}= 0.04m, with ASTSMC control while with the fixed gain STSMC controller, the measured errors are as follows: e_{XF1}= 0.18m, e_{YF1}= 0.25m, e_{XF2}= 0.2m, e_{YF2}= 0.14m. Moreover, the settling time of XY states after the occurrence of disturbances is faster as compared to fixed gain STSMC control methods.

From the quantitative comparison here; it is concluded that the proposed ASTSMC controllers show enhanced robust behavior to the acceleration type disturbances and parametric uncertainties of the system.

APPENDIX A: SIMULINK® BLOCK MODEL AND MATLAB FUNCTION CODES

Simulink® Block Implementation:

The Block Diagram for the implementation of the model is given in the Appendix A. The different figures show the block diagram implementation of different loops of the swarm of quad-rotors. Figure 21 shows the Simulink model of three quadcopters, in which the upper model is leader and lower ones are the followers. Figures 22-29 presents the different blocks of the leader quad-rotor.

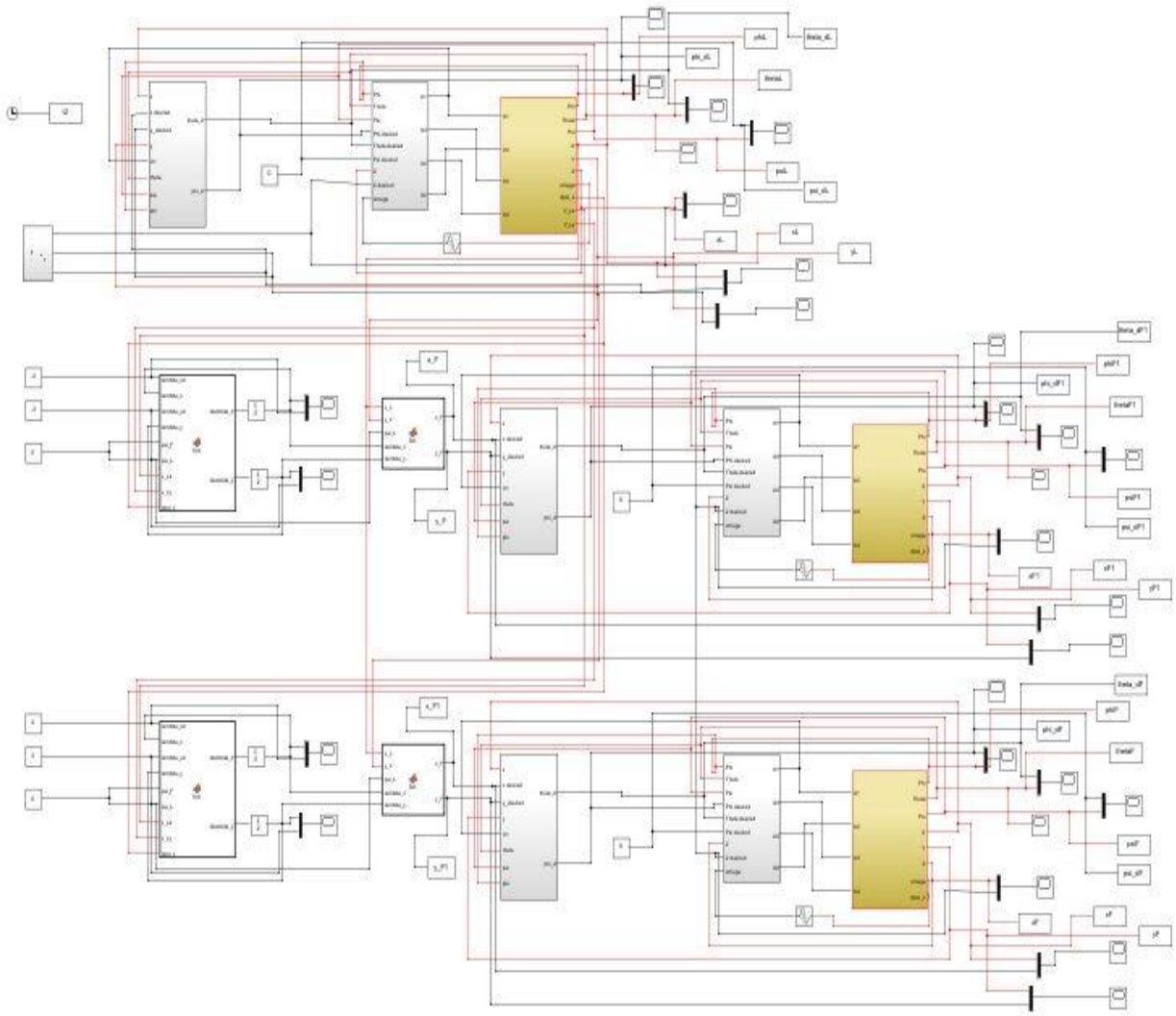

Figure 22: Simulink Model for swarm of 3 quad-copters

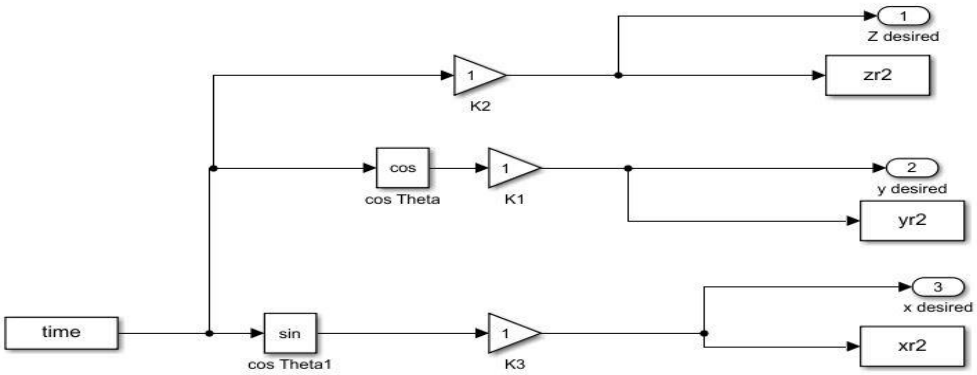

Figure 23: Reference X, Y and Z position of leader quad-copter

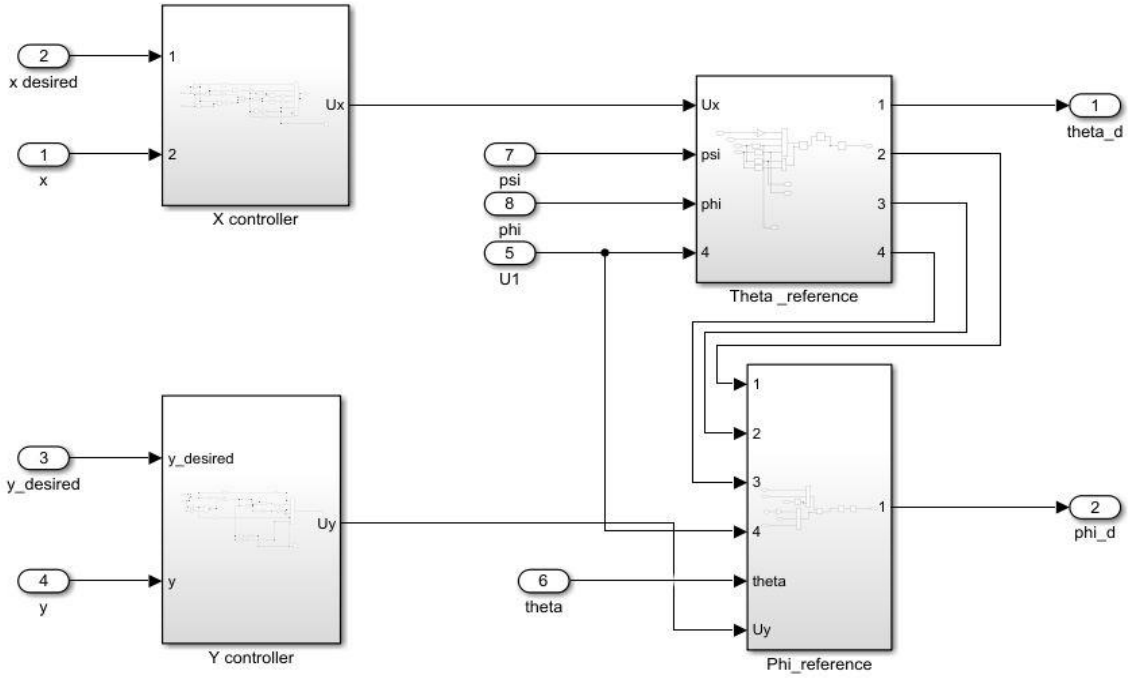

Figure 24: Position Controller for Leader quad-rotor

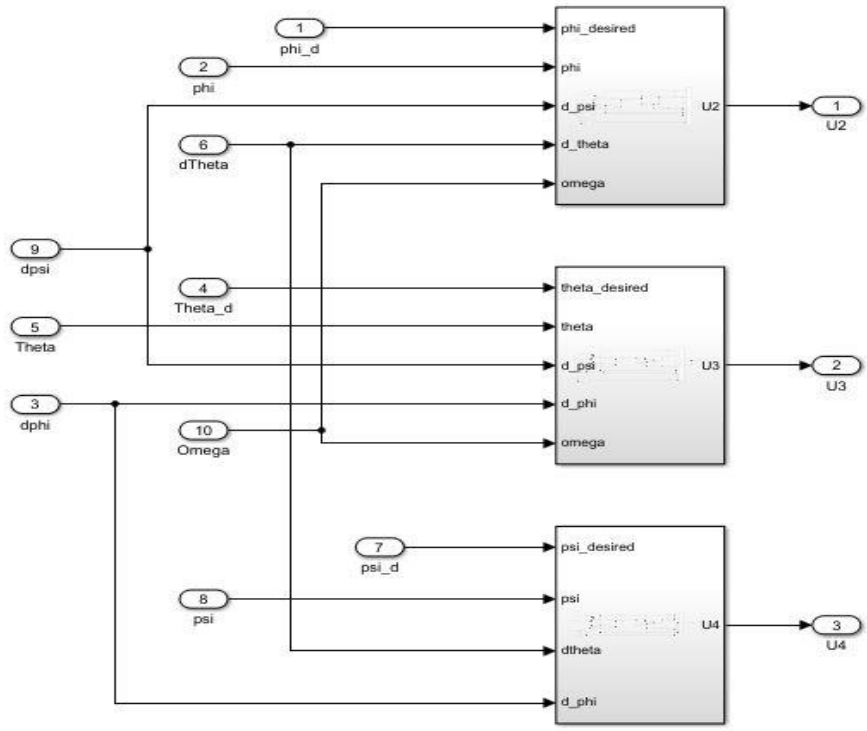

Figure 25: Attitude Controller for roll, pitch and yaw angles for leader quad-copter

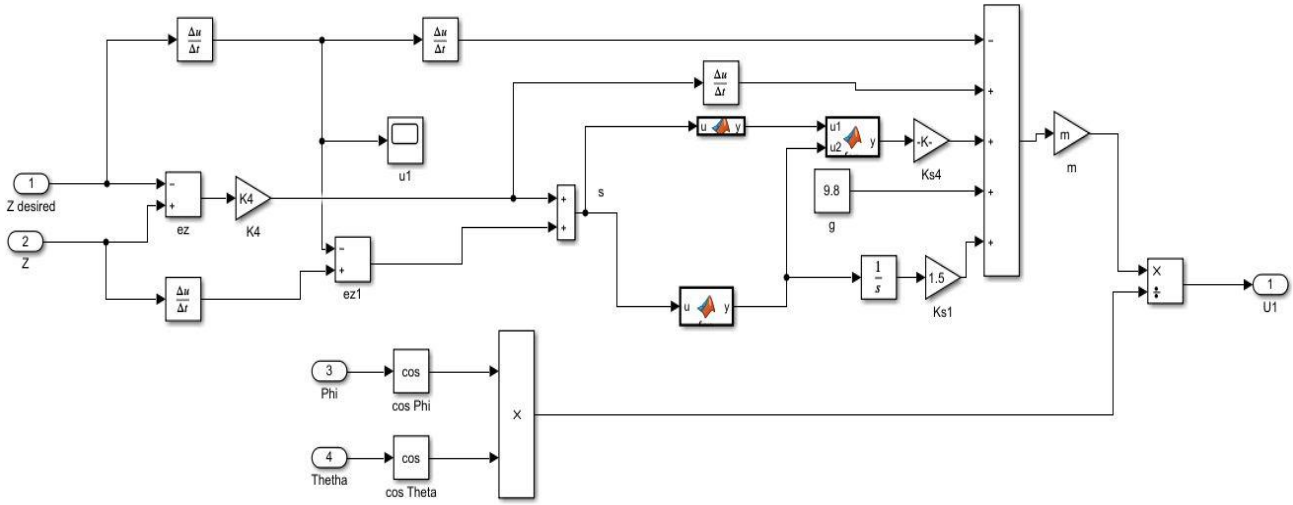

Figure 26: Altitude Controller of leader quad-copter

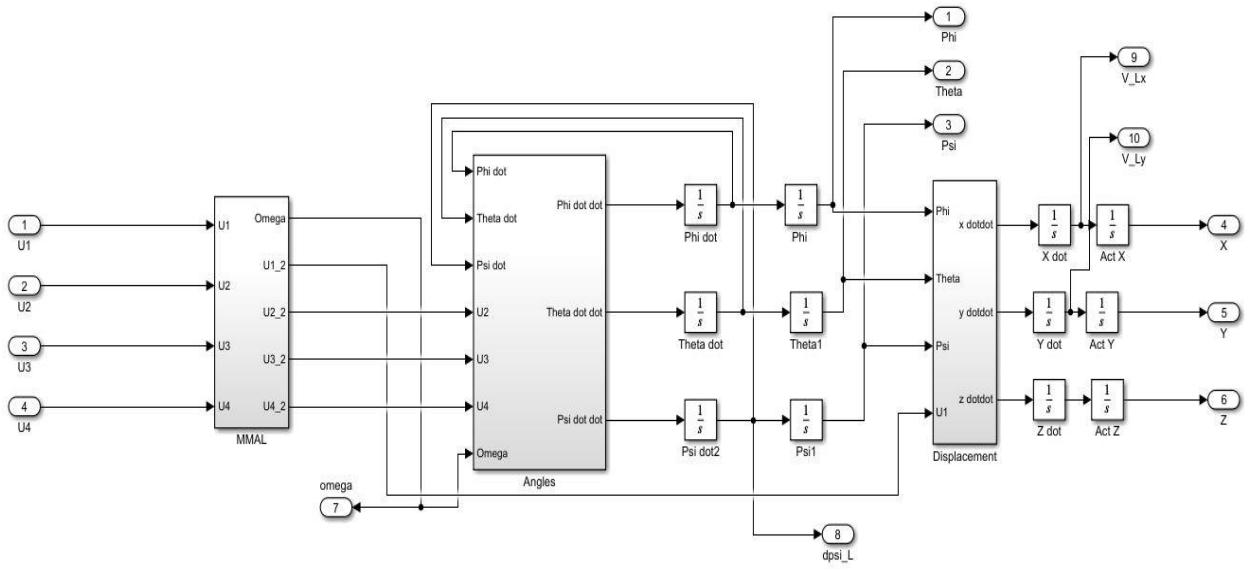

Figure 27: Dynamics model of leader quad-copter

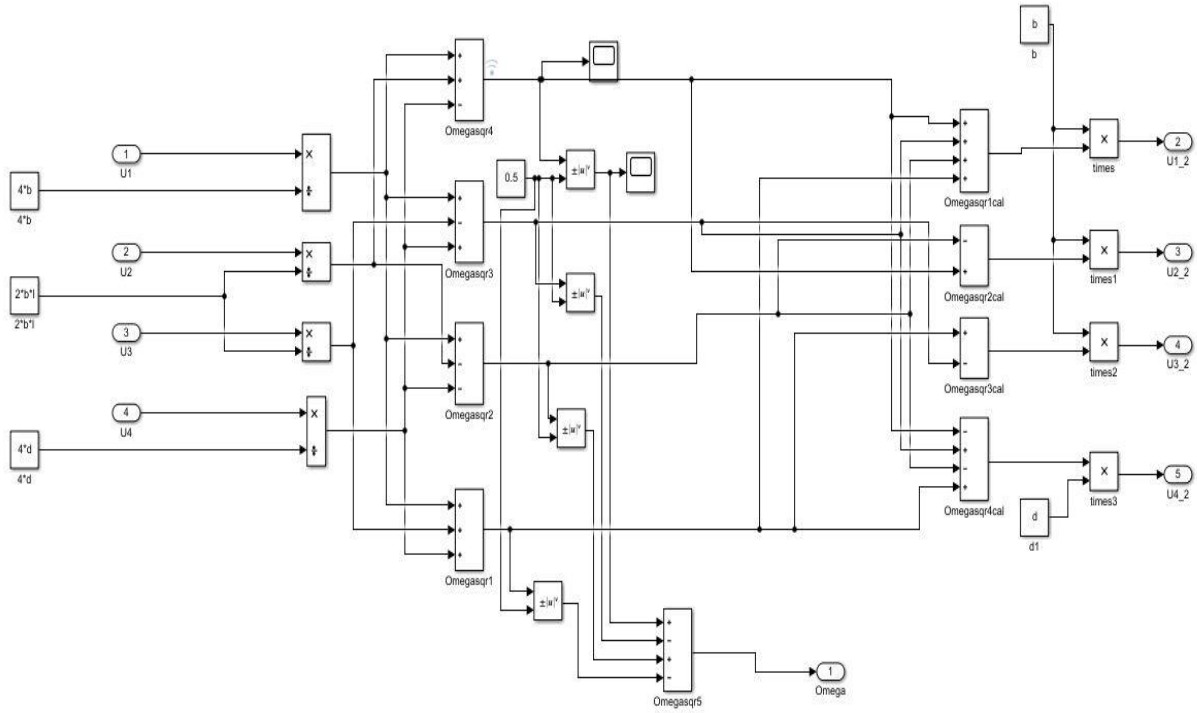

Figure 28: Motor Mixing Algorithm of leader quadcopter

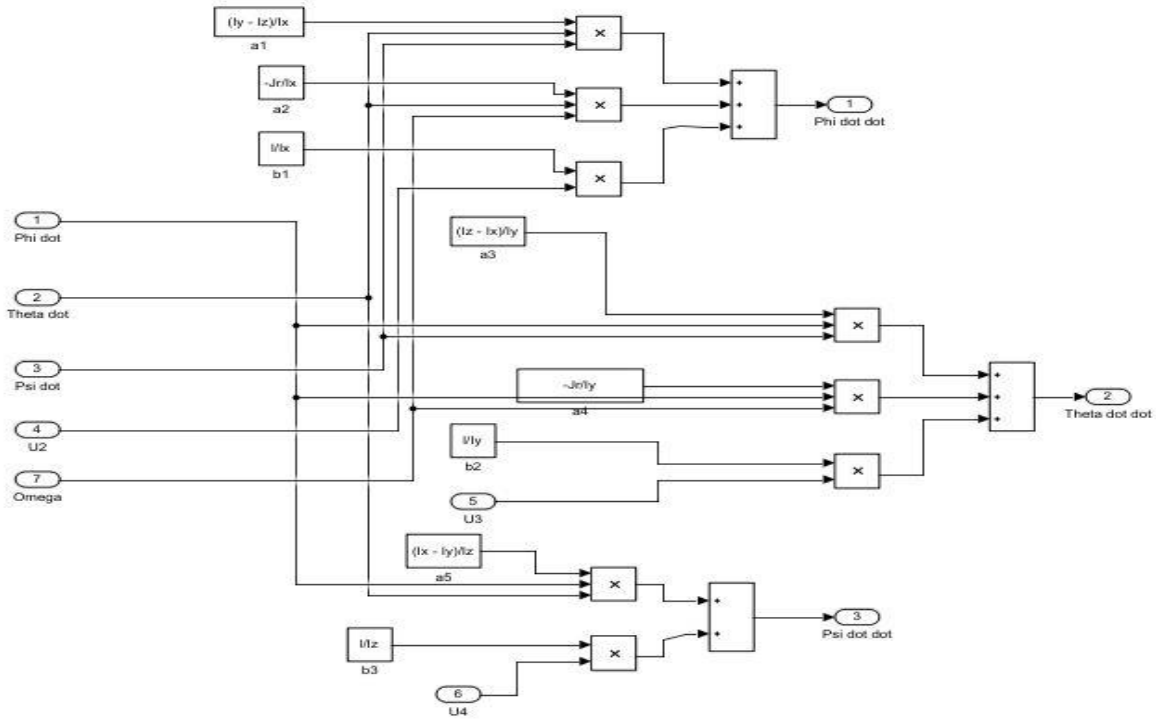

Figure 29: Rotational Dynamics of leader quadcopter

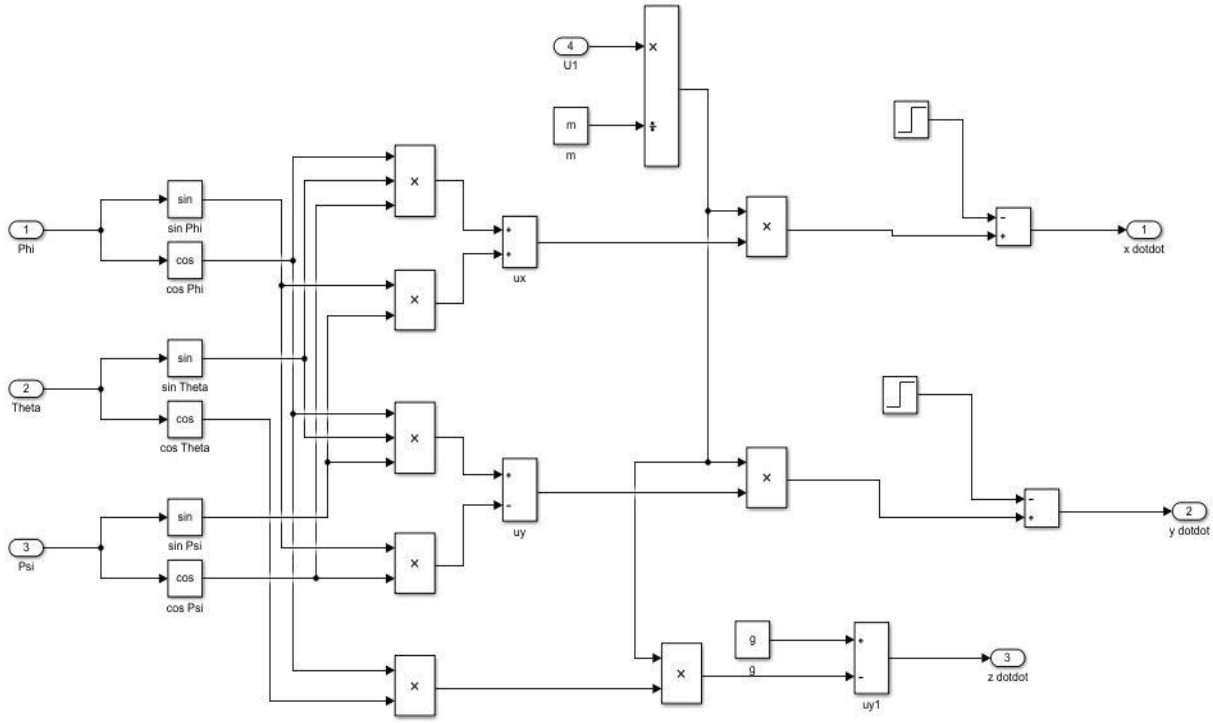

Figure 30: Translational Dynamics of leader quadcopter

MATLAB FUNCTION CODES:

The leader and follower quadcopters have the same Simulink model for position, altitude, attitude controllers and quadcopter dynamics. However, the reference position of follower quadcopters is derived from the leader quadcopter position. The MATLAB codes for the reference positions and formation errors of follower quadcopters are shown below:

Formation Error:

```
function [dlambda_x,dlambda_y]=
fcn(lambda_xd,lambda_x,lambda_yd,lambda_y,psi_F,psi_L,v_Lx,v_Ly,dpsi_L)
L=1;
kf=1;
w_L=dpsi_L;
e_x=lambda_xd-lambda_x;
e_y=lambda_yd-lambda_y;
e_psi=psi_F-psi_L;
Gamma1=v_Lx-(w_L*lambda_yd);
Gamma2=v_Ly+(w_L*lambda_xd);
invG_X=inv([-cos(e_psi) sin(e_psi) 0; -sin(e_psi) -cos(e_psi) 0; 0 0 1]);
F_X= [(e_y*w_L)+Gamma1; -(e_x*w_L)+Gamma2; e_psi];
X=[e_x;e_y;e_psi];
% fun= @(t)X ;
% integ= integral(fun);
% sigma2=X+(kf*integ);
v=invG_X*(-F_X-(kf*X));
v_Fx=v(1,1);
v_Fy=v(2,1);
w_F=v(3,1);
dlambda_x= (lambda_y*w_L)+(v_Fx*cos(e_psi))-(v_Fy*sin(e_psi))-(v_Lx);
dlambda_y= -(lambda_x*w_L)+(v_Fx*sin(e_psi))+(v_Fy*cos(e_psi))-(v_Ly);
dlambda_x=dlambda_x;
dlambda_y=dlambda_y;
```

Reference position:

```
function [x_F,y_F] = fcn(x_L,y_L,psi_L,lambda_x,lambda_y)
x_F=x_L+(lambda_x*cos(psi_L))-(lambda_y*sin(psi_L));
y_F=y_L+(lambda_x*sin(psi_L))+(lambda_y*cos(psi_L));
y1=x_F;
y2=y_F;
```

REFERENCES

[1] Shakhatreh H, Sawalmeh AH, Al-Fuqaha A, Dou Z, Almaita E, Khalil I, Othman NS, Khreishah A, Guizani M. Unmanned aerial vehicles (UAVs): A survey on civil applications and key research challenges. {\it IEEE Access}. 2019 Apr 9;7:48572-634.

[2] Research and Markets. The Global UAV Payload Market 2017– 2027. Accessed: Sep. 2020. Available: https://www. researchandmarkets.com/research/nfpsbm/the global uav

[3] Özbek NS, Önkol M, Efe MÖ. Feedback control strategies for quadrotor-type aerial robots: a survey. *Transactions of the Institute of Measurement and Control*. 2016 May;38(5):529-54.

[4] Kacimi A, Mokhtari A, Kouadri B. Sliding mode control based on adaptive backstepping approch for a quadrotor unmanned aerial vehicle. *Przeglad Elektrotechniczny*. 2012 Jan 1;88(6):188-93.

[5] Liu X, Wang H, Fu D, Yu Q, Guo P, Lei Z, Shang Y. An area-based position and attitude estimation for unmanned aerial vehicle navigation. *Science China Technological Sciences*. 2015 May 1;58(5):916-26.

[6] Dinh TX, Nam DN, Ahn KK. Robust attitude control and virtual reality model for ariquadrotor. *International Journal of Automation Technology*. 2015 May 5;9(3):283-90.

[7] Madani T, Benallegue A. Sliding mode observer and backstepping control for a quadrotor unmanned aerial vehicles. In *2007 American Control Conference* 2007 Jul 9 (pp. 5887-5892). IEEE.

[8] Alothman Y, Jasim W, Gu D. Quad-rotor lifting-transporting cable-suspended payloads control. In *2015 21st International Conference on Automation and Computing (ICAC)* 2015 Sep 11 (pp. 1-6). IEEE.

[9] Dierks T, Jagannathan S. Output feedback control of a quadrotor UAV using neural networks. IEEE transactions on neural networks. 2009 Dec 4;21(1):50-66.

[10] Cruz PJ, Oishi M, Fierro R. Lift of a cable-suspended load by a quadrotor: A hybrid system approach. In *2015 American Control Conference (ACC)* 2015 Jul 1 (pp. 1887-1892). IEEE.

[11] Mofid O, Mobayen S. Adaptive sliding mode control for finite-time stability of quad-rotor UAVs with parametric uncertainties. *ISA transactions*. 2018 Jan 1;72:1-4.

[12] Abbas R and Wu Q. Tracking Formation control for multiple Quadrotors based on fuzzy logic controller and least square oriented by genetic algorithm. Open Autom Contr Syst J 2015; 7: 842–850.

[13] Hua C, Chen J, and Li Y. Leader–follower finite-time formation control of multiple quad-rotors with prescribed performance. Int J Syst Sci 2017; 48(12): 2499–2508.

[14] Wua F, Chen J, and Liang Y. Leader–follower formation control for quadrotors. IOP Conf Series: Mater Sci Eng 2017; 187: 012016.

[15] Khaled AG and Youmin Z. Formation control of multiple quad-rotors based on leader-follower method. International conference on unmanned aircraft systems (ICUAS), Denver, CO, 2015, pp. 1037–1042.

[16] Mu B, Zhang K, and Shi Y. Integral sliding mode flight controller design for a quad-rotor and the application in a heterogeneous multi-agent system. IEEE Trans Ind Electron 2017; 64(2): 9389–9398.

[17] Mercado D A, Castro R, and Lozano R. Quad-rotors flight formation control using a leader follower approach. In: 2013 European control conference (ECC), Zurich, 2013, pp. 3858–3863.

[18] Abas MFB, Pebrianti D, Azrad S, et al. Circular leader–follower formation control of quad-rotor aerial vehicles. J Robot

[19] Li NHM and Liu HHT. Formation UAV flight control using virtual structure and motion synchronization. In: 2008 American control conference, Seattle, WA, 2008, pp. 1782–1787.

[20] Abdessameud A, Polushin IG, and Tayebi A. Motion coordination of thrust-propelled under-actuated vehicles with intermittent and delayed communications. Syst Control Lett 2015; 79: 15–22.

[21] Turpin M, Michael N, and Kumar V. Trajectory design and control for aggressive formation flight with quad-rotors. Autonomous Rob J 2012; 33(1–2): 143–156.

[22] Bayezit I and Fidan B. Distributed cohesive motion control of flight vehicle formations. IEEE Trans Ind Electron 2013; 60(12): 5763–5772.

[23] Lee D. Distributed back-stepping control of multiple thrust propeller vehicles on balanced graph. In: 18th IFAC World congress Milano (Italy), August 28 – September 2, 2011, pp. 8872–8877.

[24] Zhao W and Go HT. Quad-copter formation flight control combining MPC and robust feedback linearization. J Frankl Inst 2014; 351(3): 1335–1355. ISSN: 0016-0032.

[25] Tiago TR, Andr´e GSC, Inkyu S, et al. Nonlinear model predictive formation control for quad-copters. IFAC-Papers OnLine 2015; 48(19): 39–44. ISSN: 2405-8963.

[26] Adaptive Formation Control of Quad-rotor Unmanned Aerial Vehicles with Bounded Control Thrust. Chinese Journal of Aeronautics 2017, 30, 807–817, doi:10.1016/j.cja.2017.01.007.

[27] Ariyibi, S.; Tekinalp, O. Modeling and Control of Quadrotor Formations Carrying a Slung Load. In 2018 AIAA Information Systems-AIAA Infotech @ Aerospace; American Institute of Aeronautics and Astronautics.

[28] Rafifandi, R.; Asri, D.L.; Ekawati, E.; Budi, E.M. Leader–Follower Formation Control of Two Quadrotor UAVs. SN Appl. Sci. 2019, 1, 539, doi:10.1007/s42452-019-0551-z.

[29] Ghommam, J.; Luque-Vega, L.F.; Saad, M. Distance-Based Formation Control for Quadrotors with Collision Avoidance via Lyapunov Barrier Functions Available online: https://www.hindawi.com/journals/ijae/2020/2069631

[30] Adaptive Leader–Follower Formation Control for Swarms of Unmanned Aerial Vehicles with Motion Constraints and Unknown Disturbances. Chinese Journal of Aeronautics 2020, 33, 2972–2988, doi:10.1016/j.cja.2020.03.020.

[31] Estevez J, and Grana M. Improved control of DLO transportation by a team of quadrotors. In: Ferra´ndez VJ, A´ lvarezSa´nchez J, de la Paz LF, Toledo MJ, and Adeli H. (eds) Biomedical Applications Based on Natural and Artificial Computing. IWINAC 2017. Lecture Notes in Computer Science, vol 10338, pp. 117–126.

[32] J. A. Moreno and M. Osorio, "A Lyapunov approach to second-order sliding mode controllers and observers," 2008 47th IEEE Conference on Decision and Control, Cancun, Mexico, 2008, pp. 2856-2861, doi: 10.1109/CDC.2008.4739356.

[33] Yang, J.; Thomas, A.G.; Singh, S.; Baldi, S.; Wang, X. A Semi-Physical Platform for Guidance and Formations of Fixed-Wing Unmanned Aerial Vehicles. Sensors 2020, 20, 1136. https://doi.org/10.3390/s20041136

[34] Máthé, K.; Buşoniu, L. Vision and Control for UAVs: A Survey of General Methods and of Inexpensive Platforms for Infrastructure Inspection. Sensors 2015, 15, 14887-14916. https://doi.org/10.3390/s150714887

[35] G. Zames, “Feedback and optimal sensitivity: Model reference transformations, multiplicative seminorms, and approximate inverses,”IEEE Transactions on Automatic Control, vol. 26, no. 2, pp. 301–320, 1981.

[36] D. McFarlane and K. Glover, “A loop shaping design procedure using H infinity synthesis,” IEEE Transactions on Automatic Control, vol. 31, no. 12, pp. 1799–1819, 1992.

[37] J. C. Doyle, K. Glover, , P. P. Khargonekar, and B. A. Francis, “State space solutions to standard H2 and H infinity control problem,” IEEE Transactions on Automatic Control, vol. 34, no. 8, pp. 1228–1240, November 1989.

[38] P. Gahinet and P. Apkarian, “A linear matrix inequality approach to H∞ control,” International Journal of Robust and Nonlinear Control, vol. 4, no. 4, pp. 421–448, 1994.

[39] Edwards C, Spurgeon S. Sliding Mode Control: Theory and Applications, London: Taylor and Francis, 1998

[40] Choi HS, Park YH, Cho Y, Lee M. Global sliding mode control. IEEE Control Magazine, 2001, 21(3): 27-35.

[41] Gouaisbaut F, Dambrine M, Richard JP. Robust control of delay systems: a sliding mode control, design via LMI, Systems & Control Letters 46 (2002): 219-230.

[42] Ramirez HS, Santiago OL. Adaptive dynamical sliding mode control via backstepping, Proceedings of the 32th Conference on Decision and Control, San Antonia, Texas, December, 1992, 1422-1427.

[43] Ebrahim A, Murphy GV. Adaptive backstepping controller design of an inverted pendulum, Proceedings of the Thirty-Seventh Southeastern Symposium on System Theory, 2005, 172-174.

[44] Feng Y, Yu XH, Man ZH. Non-singular terminal sliding mode control of rigid manipulators, Automatica, 2002, 38: 2159-2167.

[45] JJE Slotine, Nonlinear applied control , W Li - Prentive Hall, Englewood Cliffs, NJ (USA), 1991.